JOC Article
pubs.acs.org/joc

Synthesis of Conformationally Locked Carba-LNAs through Intramolecular Free-Radical Addition to C=N. Electrostatic and Steric Implication of the Carba-LNA Substituents in the Modified Oligos for Nuclease and Thermodynamic Stabilities

Jianfeng Xu, Yi Liu,† Christelle Dupouy,† and Jyoti Chattopadhyaya*

Department of Bioorganic Chemistry, Box 581, ICM, Biomedical Center, Uppsala University, SE-751 23 Uppsala, Sweden. †Drs. Liu and Dupouy contributed equally to the project.

jyoti@boc.uu.se

Received May 14, 2009

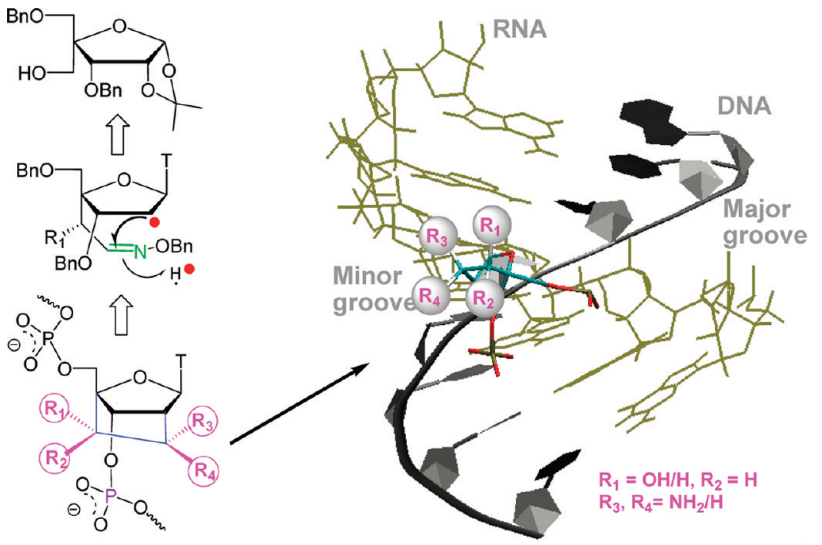

The syntheses of the hitherto unavailable parent fully unsubstituted carba-LNA and its C7′-amino and/or C6′-hydroxyl substituted derivatives, have been accomplished by the intramolecular 5-*exo* free-radical addition to a C4′-tethered C=N to give carba-LNAs with variable hydrophilic substituents at C6′/C7′ (amino and/or hydroxyl). They have been introduced into isosequential antisense oligonucleotides (AONs) to examine how their relative electrostatic and steric effects in the minor groove of a putative AON-RNA duplex affect the target affinity, nuclease resistance, and RNase H elicitation. We show that 2′-oxygen in LNA is important in stabilizing the DNA/DNA and DNA/RNA duplexes vis-à-vis the unsubstituted carba-LNA and its other derivatives and that hydrophobic groups at C6′/C7′ in both carba-LNA and carba-ENA relatively destabilize the AON/DNA duplex more profoundly than those in the AON/RNA duplexes. Two main factors affect the relative stabilities of AON/DNA versus AON/RNA duplexes: (i) hydration in the minor groove depending upon hydrophilicity vis-à-vis hydrophobicity of the substituents, and (ii) the relative size of the minor groove in the AON/DNA versus AON/RNA duplexes dictates the steric clash with the substituents depending upon their relative chiralities. We also show how the chirality and chemical nature of the C6′/C7′ substituents affect the nuclease stability as well as the thermal stability and the RNase recruitment by AON/RNA duplexes.

Introduction

Chemical modification of oligonucleotides continue to be potentially important as nucleic acid directed therapeutics, as antisense (AONs), siRNA or triplexing agents against cancer, viral, or inflammatory diseases as well as for diagnostics. Each generation of chemical modification has shown its own advantages and disadvantages. Thus, DNA phosphorothioates (PS-DNA) have been found to exhibit

Published on Web 08/11/2009 DOI: 10.1021/jo901009w

improved nuclease resistance but poor affinity to a complementary RNA.[1,2] The 2′-*O*-substituted nucleic acids in which the 2′-*O*-substituents drive the ribose to a preferential C3′-*endo* (North-type) conformation show good affinities to the RNA target.[3−5] The AONs with one or more modifications at the 3′-end with 2′-*O*-substituents, such as 2′-*O*-(3-aminopropyl)[6] or 2′-*O*-[2-[2-(*N*,*N*-dimethylamino)ethoxy]ethyl][7]), show improved nuclease resistance.[8] On the other hand, new conformationally constrained bicyclic ring systems such as LNA,[9,10] ENA,[11]and their aza-analogues (2′-amino-LNA[12] and aza-ENA[13]) are unique in that they have the continuum of the dynamic sugar pseudorotamer population locked into a fixed 3′-*endo* conformation.[14] Thus, LNA or ENA integrated oligonucleotides are preorganized to A-type canonical structure[15] and show unusually high affinity toward complementary RNA strand, but they do not have good nuclease resistance when compared to that of the PS AONs.[16]

Lately, the synthesis of a carbocyclic uridine analogue for ENA (i.e., carba-ENA-U) was reported by Nielsen′s group.[17] Although the AONs containing carba-ENA-U showed higher RNA-selective recognition compared to that of ENA,[11] no study has so far been conducted on the nuclease stability. Independently, the syntheses of the conformationally locked five-membered 7′-methyl-2′,4′-carbocyclic-LNA thymine analogue (7′-methyl-carba-LNA-T) and six-membered 7′-methyl-2′,4′-carbocyclic-ENA thymine analogue (8′-methyl-carba-ENA-T) were reported by us.[18] These unique carbocyclic 2′,4′-bridged-LNA and -ENA when incorporated into the modified AONs confer a unprecedented nuclease resistant property in the blood serum, without compromising the RNA affinity (compared to those of the isosequential LNA containing AONs), and yet they show uncompromising RNase H elicitation compared to that of the native counterpart. Moreover, the two carbon atoms in the 2′,4′-carba-bridge of carba-LNA and carba-ENA (herein defined as 6′-carbon and 7′-carbon in case of carba-LNA, and 6′-carbon and 8′-carbon in the carba-ENA derivatives) are only ∼4 Å away from the phosphate backbone of the AON/RNA heterodupex. This has led us to functionalize these two carbon atoms in the 2′,4′-carba-bridge with a bulky, hydrophobic 7′-methyl and/or hydrophilic 6′-hydroxyl group to modulate important electrostatic interactions around the phosphodiester linkage in its homo or heteroduplex form.[19] The thermal denaturation studies and stability assay of these modified AONs show that the hydrophobic nature of the 7′-methyl group and its stereochemical configuration play an important role in both the RNA affinity of modified AONs and their stabilities toward 3′-exonuclease. Whereas the stereochemical orientation of the 6′-hydroxyl group in carba-LNA does not exert a marked effect on the AON/RNA duplex thermal stability, the corresponding AONs show the chirality-dependent stability of the scissile internucleotidic phosphate toward 3′-exonuclease. A rationalization of these effects was advanced by arguing that the 7′-methyl in carba-LNA located at the center of the minor grooves could decrease the magnitude of hydration around the scissile phosphate and perturb the interaction between nuclease and phosphate linkage owing to the steric clash[20] and hydrophobic repulsion, especially when the methyl group is pointed toward the internucleotidic 3′-phosphate in the steric proximity.

We argued that it would be of considerable interest to show how the AONs containing modified carba-LNA behave in the study of RNA affinity and 3′-exonuclease stability when the hydrophobic effect of the 7′-methyl group is reversed to the hydrophilic effect upon substitution at C7′ by a positively charged amino group (i.e., 7′-amino-carba-LNA). We furthermore argued that this structure−activity study could be important if one could utilize the hitherto new parent unsubstituted carba-LNA as a reference point. Thus the synthesis of the parent unsubstituted carba-LNA and 7′-amino-carba-LNA analogues appealed to us for several reasons. First, the 7′-amino functionality could be a well-defined conjugation site in a conformationally restricted LNA-type AON.[21] Second, amine-derivatized AONs have displayed increased thermal affinities toward complementary AONs and superior nuclease resistance possibly because the introduction of positively charged moieties partially neutralized the negatively charged phosphates in the duplex at physiological pH.[22] Third, compared to 2′-amino-LNA (aza-LNA)[12] or aza-ENA,[13] the 7′-amino functionality with defined stereochemistry (*S* or *R*) at 7′-carbon will give more stereochemical information about the minor groove of AON/RNA heteroduplex, which may give more in-depth understanding

(1) Campbell, J. M.; Bacon, T. A.; Wickstorm, E. *J. Biochem. Biophys. Methods* **1990**, *20*, 259–267.
(2) Levin, A. A. *Biochim. Biophys. Acta* **1999**, *1489*, 69–84.
(3) Manoharan, M. *Biochim. Biophys. Acta* **1999**, *1489*, 117–130.
(4) Freier, S. M.; Altman, K. H. *Nucleic Acid Res.* **1997**, *25*, 4429–4443.
(5) Kawasaki, A. W.; Casper, M. D.; Freier, S. M.; Lesnik, E. A.; Zounes, M. C.; Cummins, L. L.; Gonzalez, C.; Cook, P. D. *J. Med. Chem.* **1993**, *36*, 831–841.
(6) Griffey, R. H.; Monia, B. P.; Cummins, L. L.; Freier, S.; Greig, M. J.; Guinosso, C. J.; Lesnik, E.; Manalili, S. M.; Mohan, V.; Owen, S.; Ross, B. R.; Sasmor, H.; Wancewicz, E.; Weiler, K.; Wheeler, P. D.; Cook, P. D. *J. Med. Chem.* **1996**, *39*, 5100–5109.
(7) Prhavc, M.; Prakash, T. P.; Minasov, G.; Egli, M.; Manoharan, M. *Org. Lett.* **2003**, *5*, 2017–2020.
(8) Teplova, M.; Wallace, S. T.; Minasov, G.; Tereshko, V.; Symons, A.; Cook, P. D.; Manoharan, M.; Egli, M. *Proc. Natl. Acad. Sci. U.S.A.* **1999**, *96*, 14240–14245.
(9) Singh, S. K.; Nielsen, P.; Koshkin, A. A.; Wengel, J. *Chem. Commun.* **1998**, 455–456.
(10) Koshkin, A. A.; Singh, S. K.; Nielsen, P.; Rajwanshi, V. K.; Kumar, R.; Meldgaard, M. C.; Olsen, E.; Wengel, J. *Tetrahedron* **1998**, *54*, 3607.
(11) Morita, K.; Hasegawa, C.; Kaneko, M.; Tsutsumi, S.; Sone, J.; Ishikawa, T.; Imanishi, T.; Koizumi, M. *Bioorg. Med. Chem. Lett.* **2002**, *12*, 73.
(12) Singh, S. K.; Kumar, R.; Wengel, J. *J. Org. Chem.* **1998**, *63*, 10035–10039.
(13) Varghese, O. P.; Barman, J.; Pathmasiri, W.; Plashkevych, O.; Honcharenko, D.; Chattopadhyaya, J. *J. Am. Chem. Soc.* **2006**, *128*, 15173.
(14) Obika, S.; Nanbu, D.; Hari, Y.; Morio, K.; In, Y.; Ishida, T.; Imanishi, T. *Tetrahedron Lett.* **1997**, *38*, 8735–8738.
(15) Petersen, M.; Bondensgard, K; Wengel, J.; Jacobsen, J. P. *J. Am. Chem. Soc.* **2002**, *124*, 5974–5982.
(16) Morita, K.; Takagi, M.; Hasegawa, C.; Kaneko, M.; Tsutsumi, S.; Sone, J.; Ishikawa, T.; Imanishi, T.; Koizumi, M. *Bioorg. Med. Chem.* **2003**, *11*, 2211–2226.
(17) Albak, N.; Petersen, M.; Nielsen, P. *J. Org. Chem.* **2006**, *71*, 7731–7740.
(18) Srivastava, P.; Barman, J.; Pathmasiri, W.; Plashkevych, O.; Wenska, M.; Chattopadhyaya, J. *J. Am. Chem. Soc.* **2007**, *129*, 8362–8379.
(19) Zhou, C.; Liu, Y.; Andaloussi, M.; Badgujar, N.; Plashkevych, O.; Chattopadhyaya, J. *J. Org. Chem.* **2009**, *74*, 118–134.
(20) Abdur Rahman, S. M.; Seki, S.; Obika, S.; Yoshikawa, H.; Miyashita, K.; Imanishi, T. *J. Am. Chem. Soc.* **2008**, *130*, 4886–4896.
(21) Maag, H.; Schmidt, B.; Rose, S. J. *Tetrahedron Lett.* **1994**, *35*, 6449.
(22) Cuenoud, B.; Casset, F.; Husken, D.; Natt, F.; Wolf, R. M.; Altmann, K. H.; Martin, P.; Moster, H. E. *Angew. Chem., Int. Ed.* **1998**, *37*, 1288.

on the effect of electrostatic modulation by substituents on the 2′,4′-bridge of modified carba-LNA at the center of the minor groove, compared to those of our previous result.[19]

In the previous study,[18,19] an intramolecular free-radical ring-closure reaction between a radical generated at C2′ and a distant double bond at C4′ was a key step to accomplish 7′-methyl-carba-LNA. The intramolecular 5-*exo* free-radical addition to a terminal C=C always leads however to an exocylic diastereomeric 7′-methyl group,[23] which is often difficult to manipulate for further transformation and in the past has forced us to make compromise in our structure−activity study, since 7′-methyl was a constant feature of our carba-LNA analogues. To circumvent this, we chose to initiate the 5-*exo* radical addition reaction to C=N[24−30] of an appropriately protected oximino-ether, with putative intermediate **8** or **11**, as shown in Scheme 1, for the synthesis of carba-LNAs with or without functionalization at the C6′ or C7′ of the newly formed carbocycle fused to the pentose-sugar ring to give target compounds **1**−**3** in Scheme 1. Interestingly, the benzyl-protected 7′-amino-carba-LNAs, compound **2**, can potentially be utilized as key intermediate to synthesize the parent carba-LNA **1** as outlined in Scheme 1, which simply could not be afforded by radical addition/cyclization of a radical center at C2′ to a distant double bond appended at C4′.[18,19]

We herein report the first synthesis of the parent fully unsubstituted carba-LNA and its C6′- and/or C7′-substituted derivatives, which have also led to their introduction into oligonucleotides. The thermodynamic properties of the various carba-LNA substituted oligonucleotides have been investigated by complexing with the complementary DNA or RNA, and subsequently their blood serum and 3′-exonuclease stabilities have also been investigated to assess their potential as nucleic acid directed therapeutics.

Results and Discussion

1.0. Strategy for the Synthesis of Parent Carba-LNA (1) and Its 7′-Amino (2a and 2b) and 6′-Hydroxy Analogues (3a and 3b). We argued that the oxime-ether **8** could give diastereomerically pure (*R* or *S*) 7′-amino derivatives (**2**) by a key free-radical cyclization step to a tethered C=N, and once the synthesis of 7′-amino-carba-LNA (**2**) was achieved, we could easily oxidize the 7′-amino group to a 7′-oximino and then to a 7′-keto group, which could be reduced to the 7′-hydroxy function (compound **7**) under a standard condition, which could easily give the parent carba-LNA **1** upon deoxygenation [**10** → **9** → **8** → **2** → **5** → **6** → **7** → **1**]. So in the synthesis of parent carba-LNA (**1**), 7′-amino derivative (**2**) and its oxidized products **5** and **6** may constitute key roles in our strategy. Similarly, the oxime-ether **11** was expected to give 6′-hydroxy-7′-amino derivative **3** [**14** →**13** → **12a/b** → **11** → **4** → **3**] by the key free-radical cyclization of the precursor **12b** to C=N of a tethered oximino function to engineer amino and hydroxyl functionality with both *S* and R stereochemistries. Interestingly, the key intermediates **10** and **14** could be made from the common intermediate **15**, which is already known in the literature.[13,19]

2.0. Synthesis of Diastereomerically Pure 7′-Amino-Carba-LNAs (2a-7′*R* and 2b-7′*S*). The synthetic route to the 7′-amino-carba-LNAs is shown in Scheme 2. The synthesis was started from the known precursor **10**[13] (Scheme 2). Deacetylation of **10** with 30% methylamine in methanol at rt for 1 h gave compound **16** in 95% yield. Reduction of nitrile group of **16** with DIBALH afforded the aldehyde **9** as a single product (TLC), which was directly used for the oximation[31] with *O*-benzylhydroxylamine after a simple workup procedure to give oxime **17** as a mixture of *Z* and *E* isomers (60% in two steps). After esterification of **17** with phenyl chlorothioformate, the key intermediate for radical cyclization, *δ*-functionalized *O*-benzyl oxime **18**, was provided in good yield (40% from compound **10**). The radical was generated by tin hydride reduction of the phenyl thionocarbonate **18** in toluene at reflux. Herein the oximino-ether of **18** functioned as an effective intramolecular radical trap to the 5-*exo* radical cyclization exclusively to give two enantiomerically pure stereoisomers in which the major product (60%) is **2a** (with 7′-amino at the pseudoequatorial position, 7′*R*), along with **2b** as the minor product (4%) (with the 7′*S* stereochemistry). The NMR characterizations of **2a** and **2b** have been investigated by ^{1}H, ^{13}C, as well as COSY, ^{1}H−^{13}C HMQC, long-range ^{1}H−^{13}C correlation (HMBC) experiments and 1D differential NOE experiment (Supporting Inforamtion). The attempt to cleave the N−O bond selectively with samarium diiodide[32] without affecting the 3′- and 5′-benzyl group failed. The use of 20% $Pd(OH)_2$/C and ammonium formate as a hydrogenolysis reagent at reflux temperature, however, removed the 3′- and 5′-benzyl groups easily.[19] Therefore, 10% Pd/C was used instead of 20% $Pd(OH)_2$/C at rt to reduce 7′-*N*-OBn group in **2a** and **2b** to 7′-amino without any loss of 3′- and 5′-benzyl groups; the crude higly polar putatative 7′-amino carba-LNA thus obtained was not isolated. It was subjected to trifluoroacetylation with ethyl trifluoroacetate to provide 7′-amino trifluoroacetyl protected compounds **19a/19b** (50% in two steps), which were confirmed by ^{13}C and long-range ^{1}H−^{13}C correlation (HMBC) experiments. In the ^{13}C spectrum of **19a/19b**, we observed typical quatertet peaks around 110 and 150 ppm for the trifluoroacetyl groups. $^{3}J_{HC}$ HMBC correlations between NH and the trifluoroacetyl carbonyl carbon were further used to prove the presence of 7′-trifluoroacetyl (TFA) amino functionality in compounds **19a/19b**. Debenzylation of **19a/19b** with 20%

(23) Beckwith, A. L. J.; Lawrence, T.; Serelis, A. K. *J. Chem. Soc., Chem. Commun.* **1980**, 484–485.
(24) Bartlett, P. A.; Mclaren, K. L.; Ting, P. C. *J. Am. Chem. Soc.* **1988**, *110*, 1633–1634.
(25) Martinez-Grau, A.; Marco-contelles, J. *Chem. Soc. Rev.* **1998**, *27*, 155–162.
(26) Keck, G. E.; McHardy, S. F.; Murry, J. A. *J. Am. Chem. Soc.* **1995**, *117*, 7289–7290.
(27) Dickson, L. G.; Leroy, E.; Reymond, J. L. *Org. Biomol. Chem.* **2004**, *2*, 1217–1226.
(28) Chiara, J. L.; Marco-contelles, J.; Khiar, N.; Gallego, P.; Destabel, C.; Bernabé, M. *J. Org. Chem.* **1995**, *60*, 6010–6011.
(29) Marco-contelles, J.; Pozuelo, C.; Jimeno, M. L.; Martinez, L.; Martinez-Grau, A. *J. Org. Chem.* **1992**, *57*, 2625–2631.
(30) Beckwith, A. L. J.; Schiesser, C. H. *Tetrahedron* **1985**, *41*, 3925–3941.
(31) Kumar, V.; Gauniyal, H. M.; Shaw, A. K. *Tetrahedron: Asymmetry* **2007**, *18*, 2069–2078.
(32) Marco-contelles, J.; Gallego, P.; Rodríguez-Fernández, M.; Khiar, N.; Destabel, C.; Bernabé, M.; Martinez-Grau, A.; Chiara, J. L. *J. Org. Chem.* **1997**, *62*, 7397–7412.

SCHEME 1. Retrosynthetic Analysis of the Target Compounds 1−3[a]

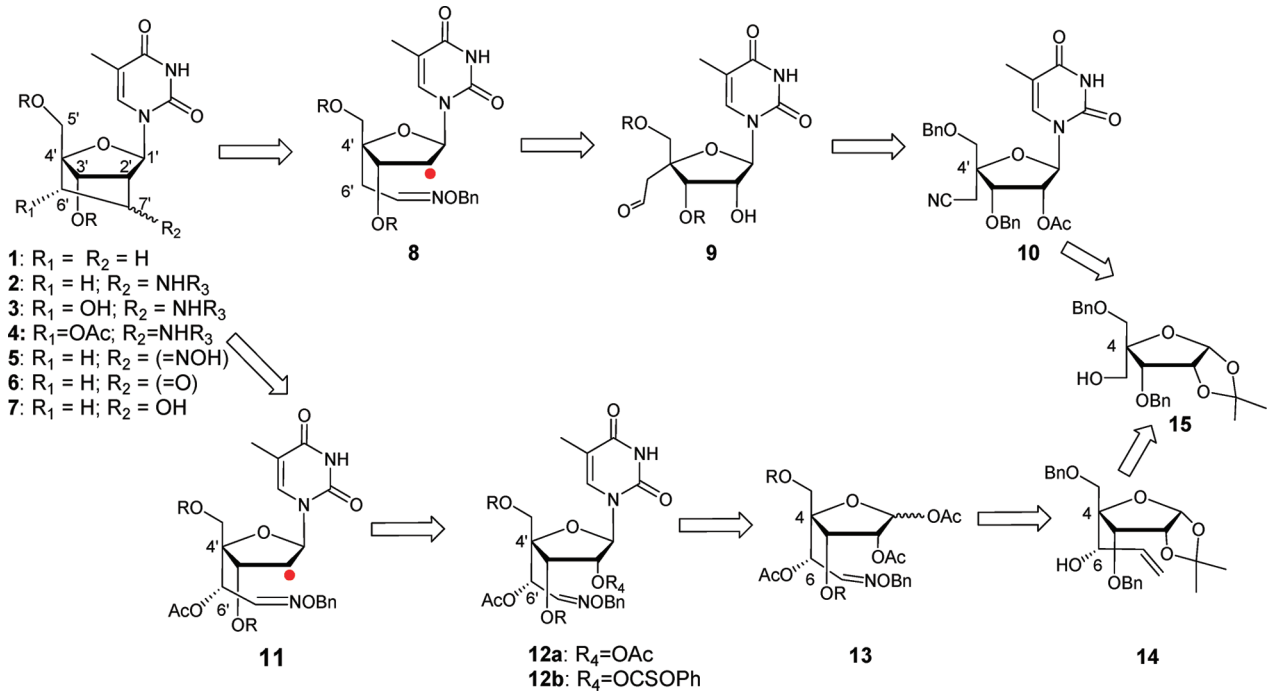

[a] R, R_1, and R_2 have been systematically varied in that R_1 = OH (OAc) or H, and R_2 = NHR_3, =NOH, =O, OH, or H [R_3 = H, OBn, TFA], and R = Bn or H or 5′-*O*-DMTr and /or 3′-phosphoramidite. When R_1 = R_2 = H (general formula, **1**), it constitutes the first synthesis of the parent unsubstituted carba-LNA.

SCHEME 2. Synthesis of Diasteromerically Pure 7′*R*- and 7′*S*-Amino-Carba-LNAs 2a/2b and Their 3′-Phosphiteamidites 21a/21b

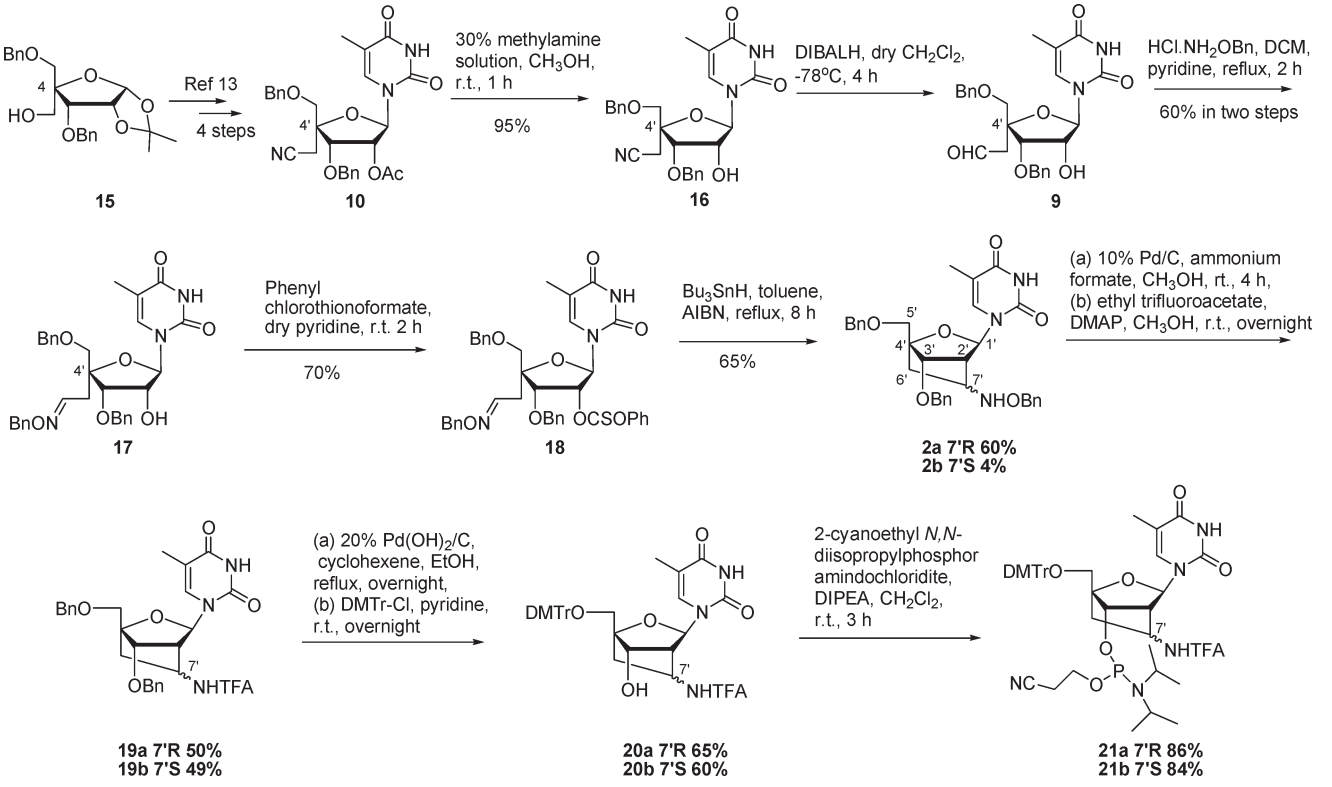

$Pd(OH)_2$/C and ammonium formate as hydrogenolysis reagents at reflux was unsuccessful as a result of the strong reactivity and poor selectivity for the benzylether group against the TFA function, which was evident by the fact

that the trifluoroacetyl functionality was also removed at reflux with these reagent. To circumvent this problem, cyclohexene[33] was used as hydrogen donor instead of ammonium formate to remove the 3′- and 5′-benzyl groups with the 7′-TFA group intact. After 5′-dimethoxytritylation and phosphitylation with 2-cyanoethyl *N*,*N*-diisopropylphosphoramindochloridite under standard conditions, phosphoramidites **21a/21b** (55% from compounds **19a/b**) were obtained as a diastereomeric mixture.

3.0. Synthesis of the Parent Carba-LNA (1). Here we have successfully utilized the major cyclic product 7′*R*-aminocarba-LNA **2a** as a key intermediate to synthesize the parent fully unsubstituted carba-LNA (Scheme 3). Oxidation of benzyloxyamine **2a** with MCPBA removed the benzyl group to give 7′-oxime **5** (60%) under a basic condition.[34,35] The structure of oxime **5** was confirmed by ^{1}H, ^{13}C, and HMBC spectrum. In the ^{1}H spectra, the peak for H7′ was not observed whereas the typical peak around 155 ppm for the oxime-carbon could be found in the ^{13}C spectra of compound **5** which shows correlations with H1′, H2′, H3′ and H6′ in the HMBC experiment. There are several methods such as hydrolytic, oxidative and reductive methods[36] to regenerate ketone from the oxime are available in the literature. For our nucleosides with complex functionalities, we have, however, chosen the mild Dess-Martin periodinane [37−39] reagent to transform the 7′-oxime **5** to 7′-ketone **6**. The reduction of ketone **6** to alcohol with $NaBH_4$ was highly stereoselective to give compound **7** (40% in two steps) with the C7′(*S*)-OH stereochemistry as the only product which was proved by strong NOE enhancement for H7′ (3.8%) ($d_{H1'-H7'} \approx 2.4$ Å) when H1′ was irradiated. The stereoselectivity for this reduction was due to the steric hindrance of bulky benzyl group at the 3′−OH which was located above the carbocycle ring and blocked the hydride attack to C7′ from the top. For the same reason, subsequent esterification of **7** with bulky phenyl chlorothioformate failed due to the unfavored orientation of hydroxyl group. Hence, sterically less bulky 7′-*O*-(methylthio)thiocarbonate[40] group in **22** was introduced, as a radical precursor instead of phenyl thionocarbonate, by the three components reaction with more reactive and less hindered reagents, CS_2 and MeI along with NaH as a proton absorbent. After the standard radical deoxygenation with tin hydride, the benzyl protected parent carba-LNA-T (**1**) was obtained in 40% yield (from compound **7**). The chemical nature of the 7′-methylene group in carba-LNA-T (**1**) was verified by DEPT and HMQC experiments. In the DEPT spectra, C7′ appeared as a secondary carbon and in the HMQC spectra, C7′ has two protons attached. The benzyl protected parent carba-LNA-T (**1**) was debenzylated through catalytic hydrogenolysis with 20% $Pd(OH)_2$ /C and ammonium formate at reflux followed by 5′-*O*-dimethoxytritylation to give **23** (70% yield in two steps), which was phosphitylated with 2-cyanoethyl *N*,*N*-diisopropylphosphoramindochloridite under standard conditions to give phosphoramidites **24** (84%) as a diastereomeric mixture.

4.0. Synthesis of Diastereomerically Pure 6′-OH/7′-NH$_2$-Carba-LNAs (3a/3b). To introduce the hydroxyl group at C6′, the synthesis was started through Grignard reaction on the aldehyde generated from the compound **15**[19] (Scheme 4) to give **14**[19] as a pure isomer with 6′*S*-OH stereochemistry. Acetylation of **14** using a mixture of acetic acid, acetic anhydride, and triflic acid gave the corresponding triacetate as an anomeric mixture. The crude triacetate was subjected to *cis*-hydroxylation with osmium tetraoxide, followed by sodium periodate cleavage of the diol to provide crude aldehyde **25**. After a simple workup, the crude aldehyde **25** was oximated with *O*-benzyl hydroxylamine in DCM and pyridine at reflux to give the corresponding 6′-substituted oxime **13** (82% from **14**). Glycosylation of **13** with thymine using a modified Vorbruggen reaction gave exclusively β-D-ribofuranosyl thymine derivatives **12a** (93%).[13] The β-configuration of compound **12a** was confirmed by 1D differential NOE experiment, which shows 4% enhancement of H6 upon irradiation of H2′ ($d_{H2'-H6} \approx 2.5$ Å for β anomer, whereas $d_{H2'-H6} \approx 5.0$ Å for α anomer). Deacetylation of **12a** using 30% methylamine in ethanol at rt gave compound **26** (96%), which was selectively esterified with phenyl chlorothioformate to give 2′-*O*-phenoxythiocarbonyl (PTC) derivatives **27** (68%). The regioselectivity of this esterification was probably due to the steric effect of the three hindered benzyl groups surrounding the 6′-hydroxyl function in **26**. In the previous study,[19] it has been shown that such an exposed hydroxyl group does not affect the nature of intramolecular 5-hexenyl radical cyclization leading to the key carbocyclic compound. In this work, however, it was found that the unprotected 6′-hydroxyl group in **27** indeed affects the 5-hexenyl radical cyclization process to C=N of an oximinoether in that we recovered 80% starting material intact and the rest of the material (20%) was decomposed to an inseparable mixture. Hence, compound **27** was protected with an acetyl group with acetic anhydride in dry pyridine to provide the key radical precursor **12b** (81%) for the radical cyclization. Thus, the 5-*exo* free-radical cyclization reaction of **12b** went on smoothly in refluxing anhydrous toluene, using AIBN as the initiator to give two diastereomerically pure compounds, in which the major product (34%) is **4a** (with 6′*S* and 7′*S* stereochemistries), along with **4b** as the minor product (24%) (with 6′*S* and 7′*R* stereochemistries). To circumvent the migration of 6′-*O*-acetyl group to 7′-amino, the 6′-*O* acetyl group was first removed with 30% methylamine before the deprotection of 7′-amino with 10% Pd/C and ammonium formate. After trifluoroacetylation of the resulting free 7′-amino group, the 6′-hydroxyl group was reprotected with acetyl to give **29a/29b** (40% from compound **4a/b**), which were debenzylated with 20% $Pd(OH)_2$, using cyclohexene as hydrogen donor. In this strategy, both 6′-*O*-acetyl and 7′-*N*-trifluoroacetyl could be kept intact during hydrogenolysis of the benzyl group. So cyclohexene can serve as a mild hydrogen donor compared to ammonium formate to give much improved selectivity for *O*-benzyl group deprotection vis-à-vis a TFA-amide group. After 5′-*O*-dimethoxytritylations and phosphitylations with 2-cyanoethyl *N*,*N*-diisopropylphosphoramindochloridite, the 6′-hydroxyl-7′-amino-carba-LNA amidite

(33) Hanessian, S.; Liak, T. J.; Vanasse, B. *Synthesis* **1981**, 396–397.
(34) Simpkins, N. S.; Stokes, S. *Tetrohedron Lett*. **1992**, *33*, 793–796.
(35) Simpkins, N. S.; Stokes, S.; Whittle, A. J. *J. Chem. Soc., Perkin Trans. 1* **1992**, 2471–2477.
(36) Corsaro, A.; Chiacchio, U.; Pistarà, V. *Synthesis* **2001**, *13*, 1903–1931.
(37) Bose, D. S.; Narsaiah, A. V. *Synth. Commun*. **1999**, *29*, 937–941.
(38) Chaudhari, S. S.; Akamanchi, K. G. *Tetrohedron Lett*. **1998**, *39*, 3909–3212.
(39) Chaudhari, S. S.; Akamanchi, K. G. *Synthesis* **1998**, *5*, 760–764.
(40) Mereyala, H. B.; Pola, P. *Synth. Commun*. **2002**, *32*, 2453–2458.

SCHEME 3. Synthesis of Fully Unsubstituted Parent Carba-LNA 1 and 5′-*O*-DMTr-3′-Phosphiteamidites 24

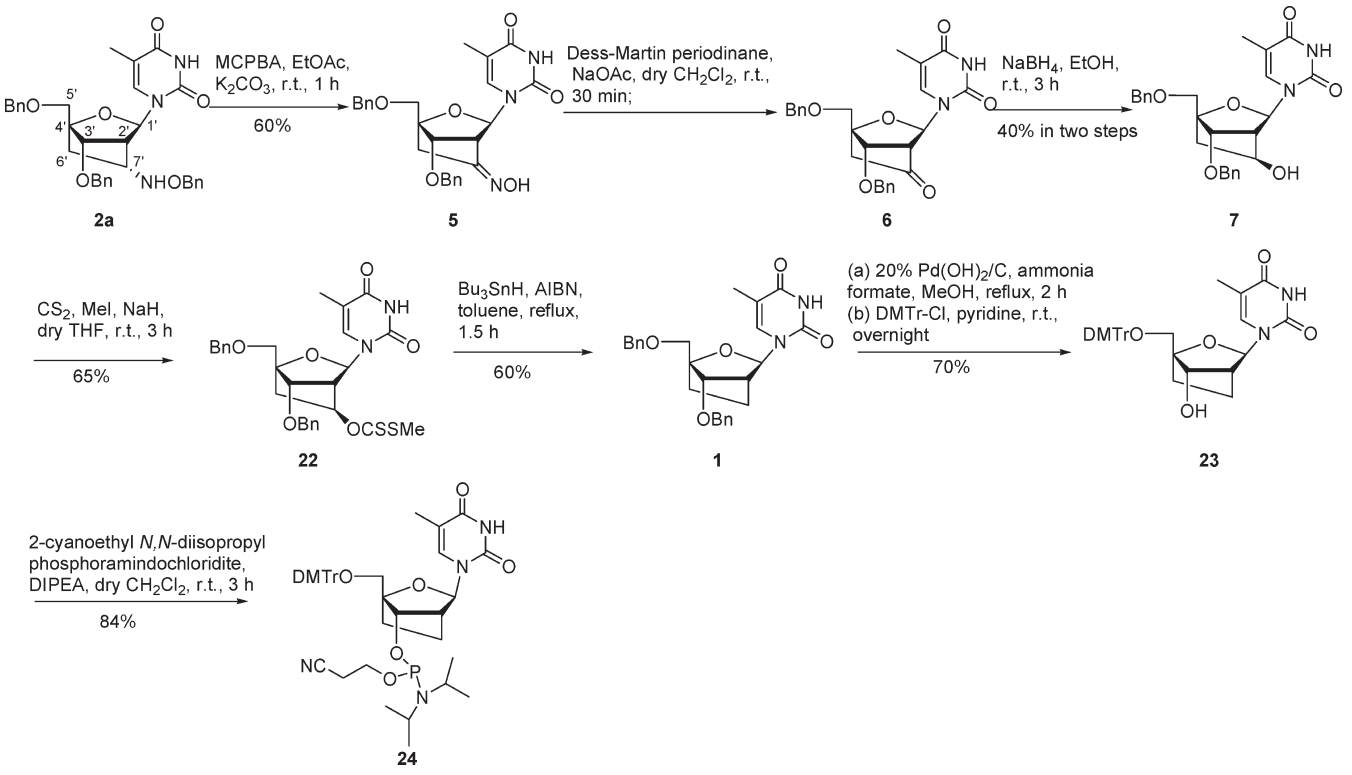

derivatives **31a/31b** (56% from compounds **29a/b**) were afforded.

5.0. NMR Characterization of Key Fused Carbocyclic Nucleoside Intermediates Involved in the Synthesis. All intermediates and final products were characterized by ^{1}H, ^{13}C, COSY, $^{1}H-^{13}C$ HMQC, HMBC and mass spectroscopy [see Supporting Information].

That the key radical ring-closure reaction successfully gives the fused carbocyclic products has been proven by 2D proton−proton and proton−carbon correlation experiments. Thus, the $^{3}J_{HC}$ HMBC correlations between H1′ and C7′ in compound **2a/b** (SI.34 for compound **2a**, SI.40 for compound **2b**) (in Scheme 2) and **4a/b** (SI.117 for compound **4a**, SI.122 for compound **4b**) (in Scheme 4) proved that the oxa-bicyclo [2.2.1] heptane ring systems have indeed been formed during radical cyclization. This five-membered ring systems in compound **2a** and **4a** were further confirmed by observation of $^{3}J_{HH}$ correlations between H2′ and H7′ ($^{3}J_{2',7'}$ = 4.2 Hz for compound **2a** and $^{3}J_{2',7'}$ = 4.0 Hz for compound **4a**), whereas the $^{3}J_{HH}$ correlations of compound **2b** and **4b** were not observed in the COSY spectrum (SI.38 for compound **2b**, SI.120 for compound **4b**) since the $^{3}J_{2',7'}$ were very close to 0 Hz, which suggested that the torsion angle H2′−C2′−C7′−H7′ was close to 90°, corroborating the 7′*S* configuration in compound **2b** and the 7′*R* configuration in compound **4b** (both of their amino groups point, however, at the 3′-phosphate). The relative configurations of C7′ in compounds **2a/b** and **4a/b** were also confirmed by 1D differential NOE experiments (Figure 1). For compound **2a**, irradiation of H1′ leads to NOE enhancement for H2′ (1.8%) ($d_{H1'-H2'} \approx 2.8$ Å) and NH (0.6%) ($d_{H1'-NH} \approx 3.4$ Å), but none for H7′ ($d_{H1'-H7'} \approx 3.8$ Å), suggesting C7′ is in 7′*R* configuration. As for compound **2b**, irradiation of H1′ leads to strong NOE enhancement for H7′ (5.3%) ($d_{H1'-H7'} \approx 2.3$ Å), suggesting C7′ is in 7′*S* configuration. For compound **4a/b**, the configuration of C6′ was determined at the Grignard reaction stage and was found[19] to have 6′*S* configuration. The configuration of C7′ was also determined by 1D NOE experiment as well as by the evaluation of coupling constants using a Karplus-type equation. For compound **4a**, irradiation of H1′ leads to 1.9% NOE enhancement for NH ($d_{H1'-NH} \approx 2.1$ Å), but none for H7′ ($d_{H1'-H7'} \approx 3.8$ Å), whereas irradiation of H7′ leads to 5.4% NOE enhancement for H6′ ($d_{H6'-H7'} \approx 2.3$ Å), suggesting that H6′ and H7′ were in *cis* disposition, which is consistent with the coupling constants ($^{3}J_{6',7'}$ = 9.5 Hz, hence dihedral angle for H6′−C6′−C7′−H7′ ≈ 18°). As for compound **4b**, strong NOE enhancement for H7′ (4.9%) ($d_{H1'-H7'} \approx 2.3$ Å) was observed when H1′ was irradiated, suggesting C7′ is in 7′*R* configuration which was further supported by the observation of the four-bond W-coupling (^{w}J) between H3′ and H7′ ($^{w}J_{3',7'}$ = 2 Hz). The relatively smaller coupling constant between H6′ and H7′ ($^{3}J_{6',7'}$) is 3 Hz, and hence dihedral angle for H6′−C6′−C7′−H7′ ≈ 113°, suggesting that H7′ and H6′ are in *trans* disposition. The coupling constants for all cyclic compounds were obtained by H−H homodecoupling experiments (SII.11−22) and found to corroborate very well with the results obtained by the NOE experiments (SII.3−10).

6.0. Stereoselectivity of the Radical Ring-Closure Reaction. The preference of the 5-hexenyl radical to orchestrate the *exo* cyclization over the *endo* mode can be explained by the preferred formation of a chairlike transition state, which suggests that radical ring closures are subject to stereoelectronic and kinetic control rather than thermodynamic control.[41]

(41) Beckwith, A. L. J. *Tetrohedron* **1981**, *37*, 3073–3100.

SCHEME 4. Synthesis of Diasteromerically Pure 6′*S*-Hydroxyl-7′*R*- or -7′*S*-Amino-Carba-LNAs 3a/3b and their 5′-*O*-DMTr-3′-Phosphiteamidites 31a/31b

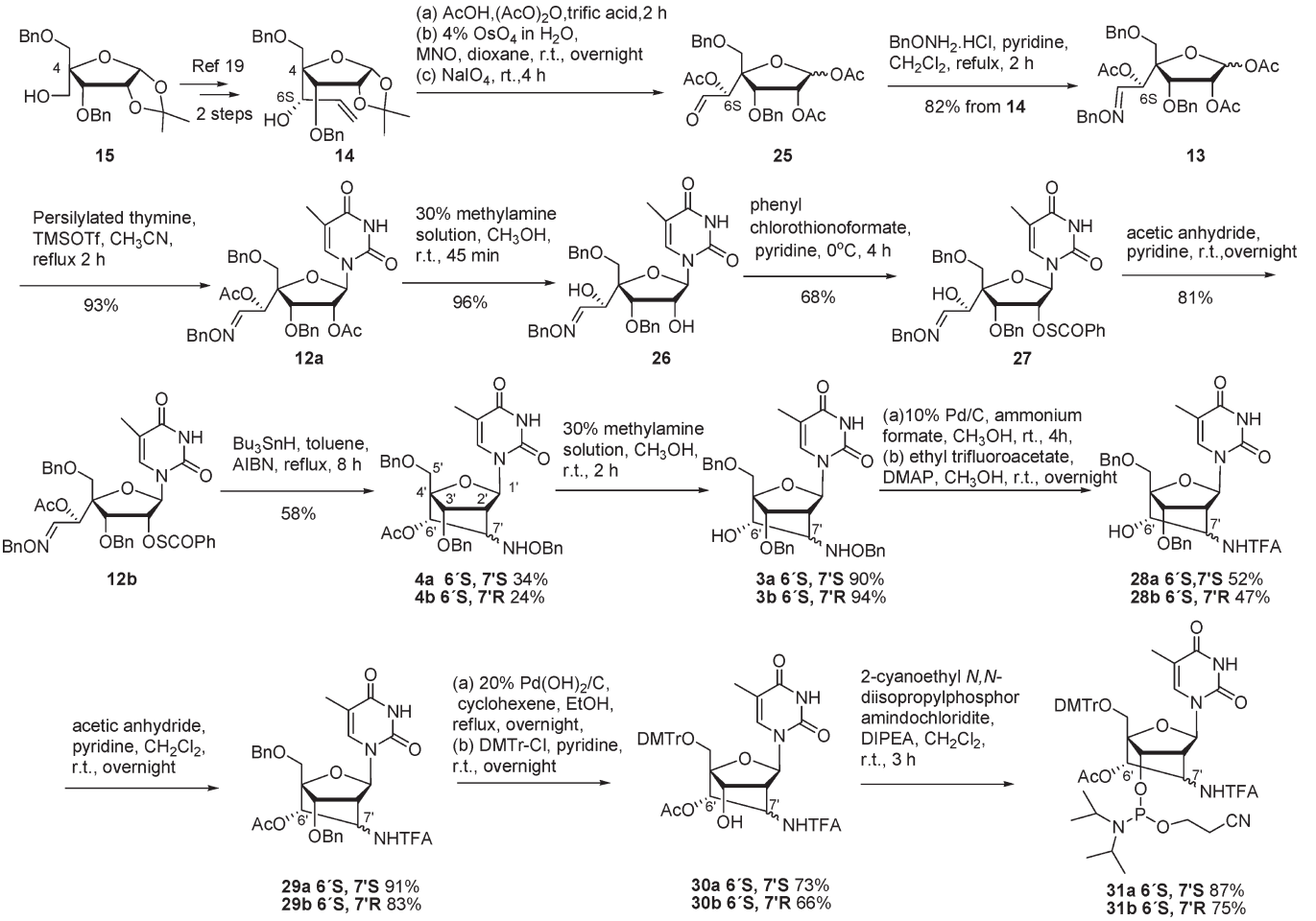

Beckwith et al. have found that 5-hexenyl intramolecular radical addition took place via cyclopentylcarbinyl radical intermediate rather than relatively more stabilized cyclohexyl radical because of unfavorable nonbonding interaction, destabilizing the transition state for 1,6-ring closure.[30,41] The preference for the *exo* mode in oximino-ether cyclization is even more profound, probably because of the additional stabilization of the aminyl radical intermediate by the lone pair of the adjacent oxygen atom. So, no cyclic product was found to have formed in our studies through the *endo* mode. The intermediate aminyl radical preferentially adopts a chairlike conformation with the substituents in the pseudoequatorial orientations to avoid the 1,3-diaxial interaction, giving 1,5-*cis* product as the major diastereomer.[24] However, the yield and stereoselectivity in this process is very structure-dependent.[29] The substitution of 5-hexenyl radical and 5-oximinoakyl radical can impact the stereoselectivity by destabilizing the chairlike conformation by nonbonding/steric interaction. In our case, the radical cyclic addition reaction to the oximino-ether were carried out with two different substrates (**18** and **12b**) as shown in Scheme 5. Both of the radical reaction proceeded as *exo* mode to adopt an energetically favored chairlike conformation in the transition states (TS1, TS2, TS3, TS4). As for compound **18**, the participation of TS1 involves a higher energy penalty because the pseudoaxial orientation of bulky *O*-benzyl hydroxylamino leads to 1,3-diaxial interaction with the bulky 3′-*O*-benzyl group, which gives a transition state with cisoid disposition of two bulky *O*-benzyl hydroxylamino and 3′-*O*-benzyl groups. As a result, the participation of TS1 is energetically disfavored, which only leads to the formation of the minor product **2b** with 7′*S* configuration. In contradistinction, TS2 transition state is energetically favored because of the pseudoequatorial orientation of *O*-benzyl hydroxylamino group leading to a transoid disposition of two bulky *O*-benzyl hydroxylamino and 3′-*O*-benzyl groups, which favors the formation of **2a** (7′*R* configuration) as a major product. These explanations are neatly corroborated by our experimental observation in that the ratio of isolated and pure *cis* product **2a** versus *trans* product **2b** is 15:1. For the cyclization of the radical intermediate, compound **12b**, there are also two transition states (cisoid-TS3 and transoid-TS4) possible to give two products with two opposite stereochemistries at C7′. However, compared to **18**, the preference of transoid stereoselectivity of radical cyclization reaction of compound **12b** is considerably reduced compared to cisoid radical cyclization, which is evidenced by the experimentally isolated yields, **4a**/**4b** = 1.4:1, respectively. The reason for the reduced influence of the transoid transition state of the radical cyclization is most probably because of the presence of asymmetric induction effect of the C6′ chirality, which makes this reaction overall less stereoselective. In the favored transition state TS4, due to the presence of 6′*S*-*O*-acetyl, 1,2-cis repulsion between acetoxy and 7′-*O*-benzyl hydroxylamino

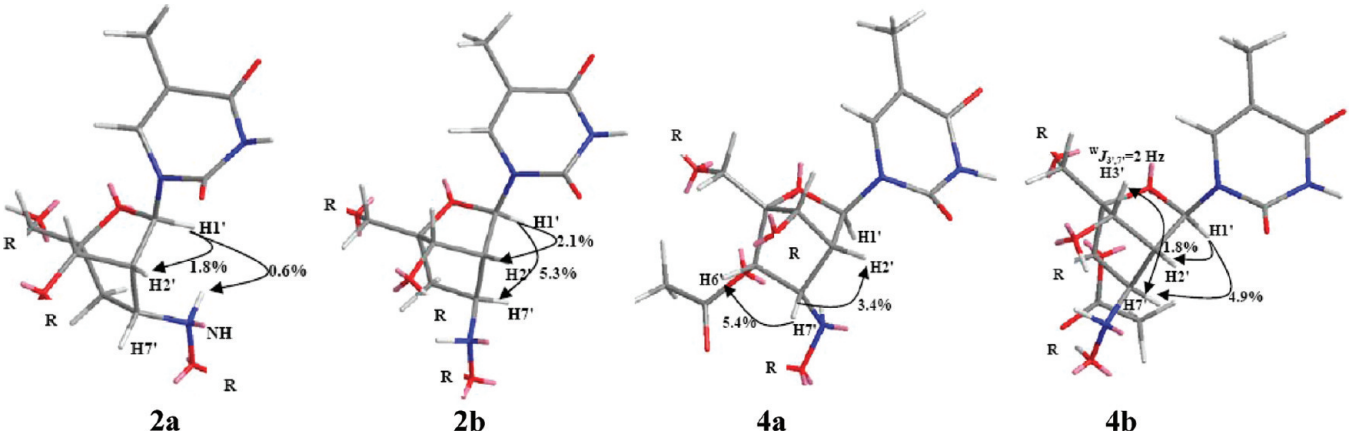

FIGURE 1. Key NOE contacts of carbocyclic compound (**2a/b**, **4a/b**) and the observation of the four-bond W-coupling (^{w}J) between H3′ and H7′ ($^{w}J_{3',7'}$ = 2 Hz) in compound **4b**. R = Bn.

SCHEME 5. Mechanism for the Stereoselectivity of the 5-*exo* Radical Ring-Closure Reaction to a Tethered −C=N

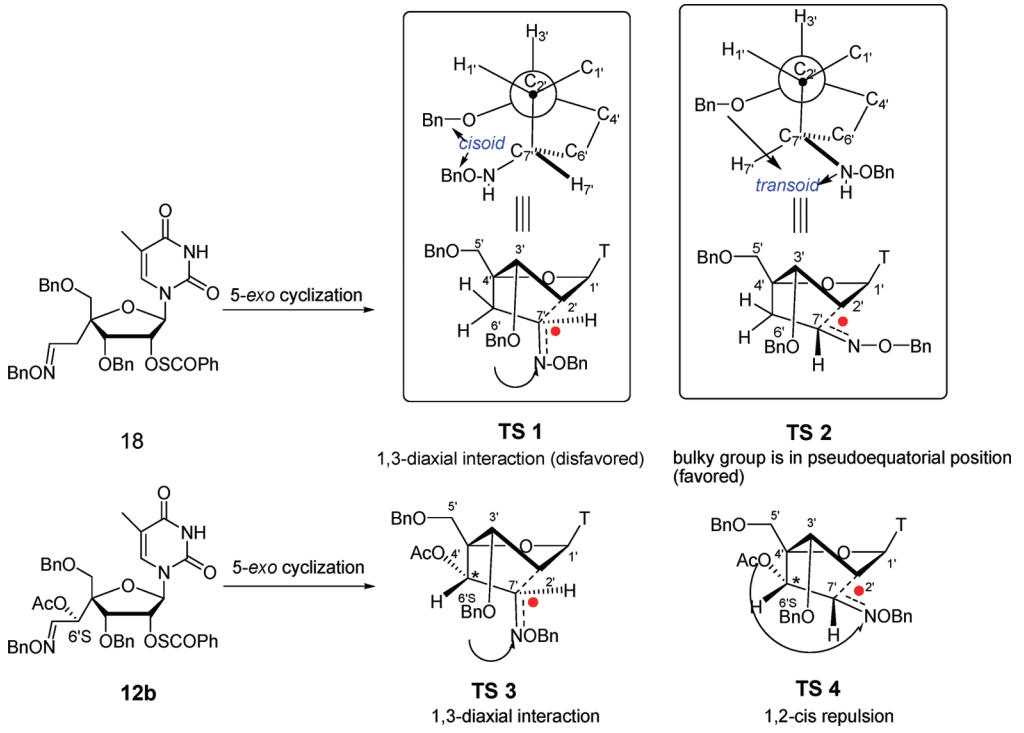

makes TS4 relatively less favored compared to TS2, although the bulky *O*-benzyl hydroxylamino is in pseudoequatorial orientation for both cases. So, the stereoselectivity for cyclization of compound **12b** is decreased by an additional 1,2-*cis* repulsion between 6′-acetoxy and 7′-*O*-benzyl hydroxylamino groups. The foregoing discussion only emphasizes the fact that the stereoselectivity of this oximino radical cyclic addition is highly structure-dependent.

7.0. Determination of Solution Conformation by $^{3}J_{H,H}$ Coupling Constants at 600 MHz (^{1}H). The parent and hydroxyl/amino-substituted carba-LNA nucleosides have been investigated in silico using ab initio calculations. The geometry optimizations of the modified nucleosides have been carried out by GAUSSIAN 98 program package[42] at the Hartree−Fock level using 6-31G**. Relevant calculated $^{3}J_{H,H}$ have been back-calculated from the corresponding theoretical torsions employing the Haasnoot−de Leeuw−Altona generalized Karplus equation[43−45] taking β substituent correction into account (see Table SII.2 in Supporting Information).

The pseudorotational phase angle (*P*) is a key parameter for the conformational analysis of sugar moiety. If the sugar moiety adopts the North-type conformation (C_3'-*endo*), the *P* value equals −1° to 34°.[46] As is shown in Table SII.2, the

(42) Frisch, M. J. et al. *Gaussian 98* (*Revision A.6*); Gaussian, Inc.: Pittsburgh, PA, 1998.

(43) Haasnoot, C. A. G.; de Leeuw, F. A. A. M.; Altona, C. *Tetrahedron* **1980**, *36*, 2783–2792.
(44) Altona, C.; Sundaralingam, M. *J. Am. Chem. Soc.* **1972**, *94*, 8205–8212.
(45) Huggins, M. L. *J. Am. Chem. Soc.* **1953**, *75*, 4123–4126.
(46) De Leeuw, H. P. M.; Haasnoot, C. A. G.; Altona, C. *Isr. J. Chem.* **1980**, *20*, 108–126.

TABLE 1. Thermal Denaturation of Duplexes of the Native, Parent Unsubstituted Carba-LNA, 6′- and 7′-Substituted Carba-LNAs, and LNA Modified AONs with Complementary RNA or DNA[a]

Entry	Modified LNA Structures **Types I - IX**	AON-Sequence* *[Encompassing modifications in the minor groove]*	With DNA ΔT_m	Minor groove Average ΔT_m(aver) in AON/DNA	With RNA ΔT_m	Minor Groove Average ΔT_m(aver) in. AON/RNA	RNA target selectivity *In AON/RNA duplex*
AON1	Native	5′-d (CTT CAT TTT TTC TTC)	Ref.*		Ref.*		
AON2	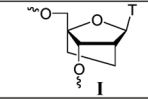 **I**	5′-d (CTT CAT TTT TTC ***T***TC)	+0.6		+3.5		+2.9
AON3		5′-d (CTT CAT TTT ***T***TC TTC)	-0.8	**-1.0**	+3.8	**+3.6**	+4.6
AON4		5′-d (CTT CAT T***T***T TTC TTC)	-1.9		+3.7		+5.6
AON5		5′-d (CTT CA***T*** TTT TTC TTC)	-2.1		+3.2		+5.3
AON6	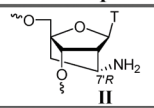 **II**	5′-d (CTT CAT TTT TTC ***T***TC)	+1.7		+2.6		+0.9
AON7		5′-d (CTT CAT TTT ***T***TC TTC)	+1.4	**+0.8**	+2.8	**+2.7**	+1.4
AON8		5′-d (CTT CAT T***T***T TTC TTC)	0		+2.6		+2.6
AON9		5′-d (CTT CA***T*** TTT TTC TTC)	0		+2.7		+2.7
AON10	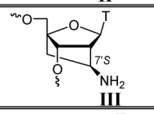 **III**	5′-d (CTT CAT TTT TTC ***T***TC)	-0.6		+0.2		+0.8
AON11		5′-d (CTT CAT TTT ***T***TC TTC)	-1.6	**-1.9**	+0.5	**+0.7**	+2.1
AON12		5′-d (CTT CAT T***T***T TTC TTC)	-2.5		+0.9		+3.4
AON13		5′-d (CTT CA***T*** TTT TTC TTC)	-2.9		+1.0		+3.9
AON14	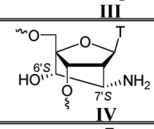 **IV**	5′-d (CTT CAT TTT TTC ***T***TC)	+1.5		+3.5		+2.0
AON15		5′-d (CTT CAT TTT ***T***TC TTC)	+1.0	**+0.4**	+3.5	**+3.4**	+2.5
AON16		5′-d (CTT CAT T***T***T TTC TTC)	-0.5		+3.0		+3.5
AON17		5′-d (CTT CA***T*** TTT TTC TTC)	-0.5		+3.5		+4.0
AON18	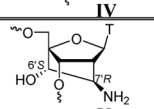 **V**	5′-d (CTT CAT TTT TTC ***T***TC)	-0.5		+1.0		+1.5
AON19		5′-d (CTT CAT TTT ***T***TC TTC)	-1.5	**-1.8**	+1.5	**+1.5**	+3.0
AON20		5′-d (CTT CAT T***T***T TTC TTC)	-2.0		+1.5		+3.5
AON21		5′-d (CTT CA***T*** TTT TTC TTC)	-2.0		+2.0		+4.0
AON22	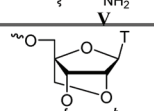 **VI**[b]	5′-d (CTT CAT TTT TTC ***T***TC)	+2.0		+4.0		+2.0
AON23		5′-d (CTT CAT TTT ***T***TC TTC)	+1.5	**+1.2**	+5.0	**+4.5**	+3.5
AON24		5′-d (CTT CAT T***T***T TTC TTC)	+0.3		+4.8		+4.5
AON25		5′-d (CTT CA***T*** TTT TTC TTC)	+1.1		+4.1		+3.0
AON26	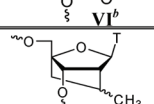 **VII**[b]	5′-d (CTT CAT TTT TTC ***T***TC)	0		+2.3		+2.3
AON27		5′-d (CTT CAT TTT ***T***TC TTC)	-1.8	**-1.7**	+3.4	**+3.1**	+5.2
AON28		5′-d (CTT CAT T***T***T TTC TTC)	-1.7		+3.5		+5.2
AON29		5′-d (CTT CA***T*** TTT TTC TTC)	-3.1		+3.2		+6.3
AON30	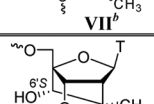 **VIII**[b]	5′-d (CTT CAT TTT TTC ***T***TC)	+1.2		+3.0		+1.8
AON31		5′-d (CTT CAT TTT ***T***TC TTC)	+1.5	**+0.4**	+4.0	**+3.8**	+2.5
AON32		5′-d (CTT CAT T***T***T TTC TTC)	+0.5		+4.1		+3.6
AON33		5′-d (CTT CA***T*** TTT TTC TTC)	-1.7		+4.0		+5.7
AON34	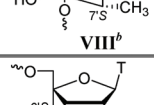 **IX**[b]	5′-d (CTT CAT TTT TTC ***T***TC)	-0.7		+1.0		+1.7
AON35		5′-d (CTT CAT TTT ***T***TC TTC)	-2.1	**-2.1**	+1.5	**+1.5**	+3.6
AON36		5′-d (CTT CAT T***T***T TTC TTC)	-3.1		+1.5		+4.6
AON37		5′-d (CTT CA***T*** TTT TTC TTC)	-2.6		+2.0		+4.6

*Molecular weights of all antisense sequences are conformed by MALDI-TOF (see Table SII.1 in Supporting Information) [a]A = 9-adeninyl, C = 1-cytosinyl, T = 1-thyminyl, ***T*** indicates the carba-LNA modified thymidine monomers with the specified structure shown in the table. "Ref." column indicates reference duplex with the native AON **1** for T_m comparison. T_m values measured as the maximum of the first derivative of the melting curve (A_{260} nm vs temperature) in medium salt buffer (60 mM tris-HCl at pH 7.5, 60 mM KCl, 0.8 mM $MgCl_2$) with temperature range 20−70 °C using 1 μM concentrations of two complementary strands. The value of T_m given is the average of two or three independent measurements (the error of the three consecutive measurements is within ±0.3 °C). ΔT_m values were obtained by comparing the T_m values of modified AONs **2**−**37** with that of the native AON **1**. The ΔT_m(aver) value obtained here is the average value for four AONs incorporated with the same compound at four different modification site. [b]Modifications of Type VI−IX have been taken from reported work,[9,18,19] and they are used for T_m comparison with our present set of modified AONs. (For more detailed comparison with all carba-LNAs and carba-ENAs, see Table SII.1 in Supporting Information.)

sugar moiety in the parent carba-LNA is indeed conformationally restricted to the North conformation [pseudorotational phase angle $P = 16.3°$, which is very similar to the value obtained for LNA ($P = 19.8°$)[18]]. Hence, the parent carba-LNA has similar affinity toward complementary RNA compared to LNA (see section 9.1). Interestingly, the chemical nature and the chirality of the substituents at 6′ and 7′ has also been found to influence puckering of the furanose sugar ring, resulting in pseudorotational angles ranging from 16° for compound **1** to 26° for compound **2a** (see Table SII.2 in Supporting Information), albeit they all adopt C_3'-*endo* conformation.

8.0. Synthesis and Purification of Carba-LNA Modified AONs 2−21. The phosphoramidites **21a/b**, **24**, and **31a/b** were incorporated as mono substitution, but at four different sites, in a 15-mer DNA sequence on an automated RNA/DNA synthesizer. Standard DNA synthesis cycle (1 μmol scale) was applied to synthesize the sequence targeted to the coding region of SV 40 large T antigen. The sequence, modification site, and structure of modification are show in Table 1. The modified building block **21a**, **24**, and **31a** gave satisfactory coupling yield (60−80%), whereas the phosphoramidites **21b** and **31b** only gave 20% of coupling yield probably due to the orientation of bulky trifluoroacetyl

amino group in **21b** and **31b**, pointing toward vicinal 3′-phosphate, blocking the coupling to some extent. Cleavage from the support and deprotection were carried out by treating the solid support with 33% aqueous ammonia at rt for 12 h to obtain the fully deprotected AONs **2**−**21**, which were purified by 20% denatured PAGE, and their structural integrity was confirmed by MALDI-TOF mass measurement (see Table SII.1 in Supporting Information). The AONs **22**−**37** containing LNA,[9,10] 7′(*S*,*R*)-methyl-carba-LNA,[18] 6′*S*-hydroxyl-7′*S*-methyl-carba-LNA,[19] and 6′*S*-hydroxyl-7′*R*-methyl-carba-LNA,[19] have been reported earlier; they were, however, used in this work for comparison to clarify the modulation effects of modified carba-LNAs in general.

9.0. Thermal Denaturation Studies of the Carba-LNA Modified AONs. The T_m values of duplex formed by AONs **2**−**37** with the complementary RNA or DNA were measured in the present study and compared with that of the native AON **1** to provide ΔT_m, which are listed in Table 1. The T_m value of duplexes formed by AONs **38**−**76** (see Table SII.1 in Supporting Information) with the complementary RNA or DNA are also cited from previous publications[18,19] on the modified carba-LNA containing AONs in order to compare and shed light on the structure−activities relationship (SAR) of all 6′/7′-modified carba-LNAs and carba-ENAs (section 9.6). Comparison of ΔT_m (SAR) of AONs containing differently modified carba-LNA derivatives clearly illustrate how the hydrophilic positively charged amino group versus the hydrophobic methyl group at C7′ vis-à-vis the hydrophilic hydroxyl group at C6′ (on the basis of the chiralities of respective substituents) affects the electrostatics, steric, and the spine of hydration around the 3′- vis-à-vis 5′-internucleotidic phosphate, thereby modulating the modified AONs affinity toward the complementary RNA or DNA, as determined by the measurement of the relative stabilities of the resulting hetero and homoduplexes. In this study, native AON (AON **1**), the parent unsubstituted carba-LNAs (AONs **2**−**5**), and LNA[9,10] (AONs **22**−**25**) were used as reference for the sake of comparison (Table 1). Throughout the present study, we have used four different single-modified AONs, each one of them encompassing the minor groove of the AON/DNA and AON/RNA duplexes, and therefore ΔT_m of all duplexes have been averaged [ΔT_m(aver)] in a separate column to reflect the average effect of all minor groove modifications (see Table 1) in general.

9.1. Comparison of Type I (Parent Carba-LNA) with Type VI (LNA). The experiments show that a single incorporation of parent carba-LNA (AON **2**−**5**) increases the stability of the duplexes formed with the complementatry RNA by 3−4 °C [ΔT_m(aver) = 3.6 °C], which means ∼1 °C decrease in ΔT_m compared to that of the LNA-incorporated isosequential AONs (compare AONs **2**−**5** with AONs **22**−**25**). The lack of hydrophilic substituent at C2′ (as in 2′-oxa group in LNA[9,10]) in the parent unsubstituted carba-LNA leads to a decrease in the heteroduplex stability with complementary RNA, suggesting that the 2′-oxygen of LNA plays an important role in the thermodynamic stability of the corresponding heteroduplex, which is supported by Egli′s work on the X-ray crystal structure of LNA duplex.[47] These workers showed that the 2′-oxa substituent of LNA is engaged in the hydrogen bonding to water molecules, which contributes to the extensive hydration network in the duplex, reducing the electrostatic repulsion of the internucleotidic phosphates, and thereby contributing to an increase in the thermodynamic stability.[48] In the context of the dsDNA duplex with carba-LNA and LNA, a net decrease of 1−2 °C in T_m [ΔT_m(aver) = −1 °C] was observed for the carba-LNA incorporated AONs (AON **2**−**5**) in the AON/DNA homoduplexes, whereas the LNA incorporated AONs (AON **22**−**25**) duplexes show 0.5−2 °C increase in T_m compared to the native AON (AON **1**). This suggests that the 2′-oxa substituent of the bicyclic moiety is much more important for the formation of stabilized B-type dsDNA than that of stabilized DNA/RNA hybrid, which was also observed in the six-membered ring systems.[17] The extent of hydration of the wider minor groove in the DNA/RNA duplex is perhaps relatively less important compared to that of the relatively narrow and extensively hydrated minor groove in B-type DNA/DNA duplex. Hence, substitution of the hydrophilic 2′-oxa substituent by the hydrophobic C2′-methylene is relatively less tolerated in the AON/DNA duplexes compared to those of the AON/RNA duplexes. This is why the carba-LNA incorporated AONs are more complementary RNA-selective by 1−2 °C/modification compared to that of the LNA counterpart.

9.2. Comparison of Type I (Parent Carba-LNA) with Type VII [7′(*S*/*R*)-Methyl-Carba-LNA]. Type VII modification [7′(*S*/*R*)-methyl-carba-LNA)] has one additional methyl group at C7′ as a diastereomeric mixture[18] (7′*R* vs 7′*S*, 7: 3 by NMR, inseparable mixture) compared to Type I (parent unsubstituted carba-LNA). The diastereomeric ratio of 7′*R* to 7′*S* in Type VII suggested that the major product (70%) with methyl group at the pseudoequatorial orientation (7′*R*) is pointing away from the vicinal 3′-phosphate ($d_{(7'S\text{-methyl})\text{-}3'P}$ ≈ 4.3 Å, $d_{(7'R\text{-methyl})\text{-}3'P}$ ≈ 5.4 Å), whereas the pseudoaxial methyl group in the 7′*S* minor product (30%) is pointing at the vicinal 3′-phosphate. As a result, the Type I modified AONs **2**−**5** have slightly higher ΔT_m(aver) = ∼0.5 °C for AON/RNA duplex compared to those of Type VII modifications (AONs **26**−**29**). This result is consistent with the previous conclusion made by Zhou et al.[19] in that when the hydrophobic 7′-methyl is pointing at the vicinal 3′-phosphate, it can impair the AON/RNA duplex thermal stability by perturbing the hydration network in the minor groove.

9.3. Comparison of Type II with Type III and Type IV with Type V Using Type I (Parent Carba-LNA) as Reference. To transform the hydrophobic nature of carba-LNA, owing to the endoxcyclic 2′-CH_2 group, in Type I to a hydrophilic substitutent to improve the hydration pattern of duplex, the amino group was introduced at C7′ with two different chiralities (*S* vs *R*), and the corresponding diastereomerically pure 7′-amino (*S* and *R*) modified carba-LNAs was incorporated into Type II and Type III modified AONs. Table 1 shows that the C7′-amino functionality in either *R* (Type II) or *S* (Type III) configuration can surprisingly destabilize the AON/RNA duplex compared to Type I modification. Type II modification decreases ΔT_m(aver) by 1 °C compared to Type I (parent carba-LNA), whereas Type III decreases

(47) Egli, M.; Minasov, G.; Teplova, M.; Kumar, R.; Wengel, J. *Chem. Commun.* **2001**, 651–652.

(48) Tereshko, V.; Gryaznov, S.; Egli, M. *J. Am. Chem. Soc.* **1998**, *120*, 269–283.

ΔT_m(aver) by up to 3 °C compared to Type I (parent carba-LNA). When the 7′-amino group points at the vicinal 3′-phosphate (i.e., 7′*S*) ($d_{C7'amino(up)\text{-}3'P} \approx 4.2$ Å for 7′*S* versus $d_{C7'amino(down)\text{-}3'P} \approx 5.4$ Å for 7′*R*), the destabilization effect on the AON/RNA duplex is more pronounced than that for 7′*R*-amino, in which the amino group points away from the vicinal 3′-phosphate, despite the fact that the distance difference between them is only ~1.2 Å, and hence the directionality of the amino function in the minor groove is important. This result can be further corroborated by the comparison of Type IV (6′*S*-hydroxyl-7′*S*-amino-carba-LNA) with Type V (6′*S*-hydroxyl-7′*R*-amino-carba-LNA) in that the 6′*S*-hydroxyl-7′*R*-amino-carba-LNA modified AONs **18**−**21** (Type V) also lower ΔT_m(aver) for the AON/RNA duplex by 2.0 °C compared to 6′*S*-hydroxyl-7′*S*-amino-carba-LNA modified AONs **14**−**17** (Type IV). The role conferred by the configuration-dependency of the C7′-amino functionality in the AON/RNA heteroduplex is perhaps owing to a possible steric effect. As for the AON/DNA duplex with a narrower minor groove, the role conferred by the configuration is more complicated. It can be seen from Table 1 that with the 7′*R*-amino carba-LNA (the C7′-amino is pointing away from the 3′-phosphate), the hydration in the minor groove of AON/DNA duplex is promoted (hence increase in ΔT_m(aver) is found compared to that of Carba-LNA), whereas with the 7′*S*-amino carba-LNA (the C7′-amino is pointing toward the 3′-phosphate), the AON/DNA duplex hydration is relatively poorer and therefore destabilizing.

9.4. Comparison of Type IV with Type VIII and Type V with Type IX. It is observed that both the hydrophilic 7′-amino group and the hydrophobic 7′-methyl group, when they are in the pseudoaxial disposition, bringing themselves in close steric proximity to the vicinal 3′-phosphate, can destabilize the duplex formed with the complementary RNA. We observed similar ΔT_m(aver) when comparing Type IV (6′*S*-hydroxyl-7′*S*-amino-carba-LNA) with Type VIII (6′*S*-hydroxyl-7′*S*-methyl-carba-LNA) and Type V (6′*S*-hydroxyl-7′*R*-amino-carba-LNA) with Type IX (6′*S*-hydroxyl-7′*R*-methyl-carba-LNA), suggesting that the hydrophilic amino and hydrophobic methyl group with the same orientation at C7′ have a similar destabilizing effect on the AON/RNA duplex. So the relative stabilities of the corresponding AON/RNA and AON/DNA duplex depend on the chiralities of the substituents at C7′.

9.5. Comparison of Type II with Type IV and Type III with Type V Modifications. Both Type IV (6′*S*-hydroxyl-7′*S*-amino-carba-LNA) and Type V (6′*S*-hydroxyl-7′*R*-amino-carba-LNA) modifications have one additional 6′*S*-hydroxyl group, which points away from the vicinal 3′-phosphate ($d_{6'S\text{-}hydroxyl\text{-}3'P} \approx 6.0$ Å versus $d_{6'S\text{-}hydroxyl\text{-}5'P} \approx 4.6$ Å), compared to Type II (7′*R*-amino-carba-LNA) modification and Type III (7′*S*-amino-carba-LNA) modification, respectively. As a result, the 6′*S*-hydroxyl group of AONs **14**−**17** (Type IV) and AONs **18**−**21** (Type V) stabilize the AON/DNA duplex by ~1 °C in ΔT_m(aver) compared to that of AONs **6**−**9** (Type II) and AONs **10**−**13** (Type III), respectively.

9.6. Structure−Activity Relationships of Modified Carba-LNA and Carba-ENA for Thermal Affinity. To fully illustrate and understand the functional modulation of the AON properties rendered by different chiral substituents at the 2′,4′-fused carbon bridge of carba-LNAs and carba-ENAs, a brief comparative discussion on the structure−activity relationships of the thermal affinities of all 13 modified carba-LNAs[18,19] and 5 modified carba-ENAs[18,19] (Figure 2) is made here. The C6′ and/or C7′ substituent of carba-LNA are close to the adjacent phosphodiester linkage (see above for discussion), which suggests that the hydration pattern, electrostatics, and steric effects around the adjacent phosphates could be modulated by introducing a hydrophobic sterically bulky methyl, hydrophilic hydroxyl, or positively charged amino group. In summary, the hydrophilic amino group and hydrophobic methyl group at 7′ in modified carba-LNA have a similar destabilizing effect on T_m, and the extent of destabilizing effects is dependent on the orientation of the substituents, suggesting that as for the 7′-substituted carba-LNA, the stabilities of DNA/RNA duplexes is determined by the orientation of the 7′-substituents regardless of their chemical nature. On the contrary, both the hydrophilic hydroxyl group and hydrophobic methyl group at C6′ in modified carba-LNA can stabilize the duplex regardless of their orientation. As for the modified carba-ENA, they all show less affinity toward the complementary RNA compared to the five-membered carba-LNA anologues. (For more detailed discussion see SII.32−33 in Supporting Information.)

9.7. Competitive Interplay of Electrostatic versus Steric Effect Dictates the Overall Stability of the AON/RNA Heteroduplexes. To explain how different hydrophilic versus hydrophobic substitutents in carba-LNAs and carba-ENAs stabilize or destabilize the T_m, we would like to address the stereochemical location of the substituents of the 2′,4′-bridge in the minor groove of the DNA/RNA duplex. In the 7′-CH_3/NH_2 substituted carba-LNAs, both the bulky hydrophobic methyl group and the hydrophilic amino group, located in the center of the minor groove of the DNA/RNA duplex, will either perturb or enhance the hydration network in the minor groove in competition with the destabilizing steric effect imparted by these groups. The steric clash resulting from the 7′-CH_3/NH_2 will lead to slight extension of the minor groove to accommodate the bulky substituents, which results in a local or global conformational change at the cost of the thermal stability. With respect to the AON/RNA duplex, the steric effect is suggested to be more prominent than the hydration effect. Hence, the hydrophilic amino group and hydrophobic methyl group with the same orientation at C7′ have a similar destabilizing effect on the DNA/RNA duplex, which has been emphasized in the discussion above. Clearly, the hydration effect and the steric effect are even more pronounced in the DNA/DNA duplexes because of their relatively narrower minor groove width compared to that of the DNA/RNA duplex, which explains why the AON/DNA duplex with 8′-CH_3-carba-ENA (Types XV−XIX) modification give a much larger decrease in T_m compared to that in the corresponding AON/RNA duplex, rendering them a good RNA recognizing agent. Compared to the 7′-substituents at carba-LNA or 8′-substituents at carba-ENA that are located at the center of the minor groove of AON/RNA duplex, substituents at 6′ of carba-LNAs and carba-ENAs are located at the border of grooves, close to the phosphate linkage. Hence, the substituent at 6′ (CH_3/OH) has a relatively smaller effect on the hydration network, which leads to less pronounced effects conferred by the C6′-substituents compared to that of C7′-substituents.

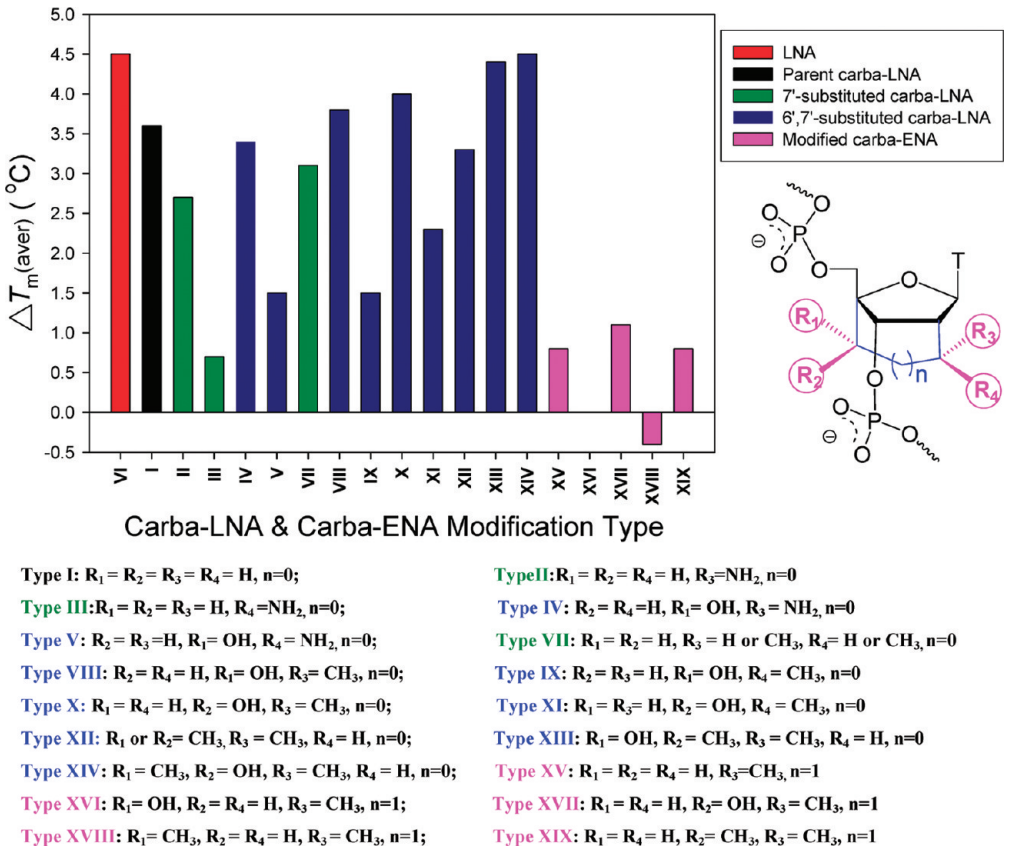

FIGURE 2. Increased thermal affinities toward RNA complements relative to that of the native AON (ΔT_m) for all modified carba-LNAs and carba-ENAs. The ΔT_m(aver) values exhibited here is the average value for four isosequential AONs in which a given modification with the same compound is incorporated at four different sites covering the minor groove (see Table 1 and Table SII.1 in Supporting Information for more detailed comparison).

10.0. 3′-Exonuclease Stability of Parent Carba-LNA Containing AONs and Modified Carba-LNA Containing AONs. The metabolism of AONs *in vivo* involves degradation by exo- and endonucleases, and the predominate nuclease activity in blood serum originates from 3′-exonuclease.[49] Hence the newly synthesized AONs (AON **2**, **6**, **10**, **14**, **18**) with a single modification at position ***T***13 (position 3 from 3′-end) were utilized to test the 3′-exonuclease stability of the modified carba-LNA AONs. The known AONs containing LNA (AON **22**), 7′(*S*,*R*)-methyl-carba-LNA (AON **26**), 6′*S*-hydroxyl-7′*S*-methyl-carba-LNA (AON **30**), and 6′*S*-hydroxyl-7′*R*-methyl-carba-LNA (AON **34**) were also used in our present parallel experiments for comparison to clarify the stabilizing effects of the modified carba-LNAs. The selected AONs were labeled at the 5′-end with ^{32}P and then incubated with phosphodiesterase I from *Crotalus adamateas* venom (SVPDE) [SVPDE 6.7 ng/μL, AON 3 μM, 100 mM Tris-HCl (pH 8.0), 15 mM $MgCl_2$, total volume 30 μL] at 21 °C. Aliquots were taken out at appropriate time intervals and analyzed by 20% denaturing PAGE. The gel pictures were obtained upon autoradiography and are shown in Figure 3A. The native DNA (AON **1**) and the LNA incorporated AON (AON **22**) did not have any 3′-exonuclease resistance and were completely degraded in ~10 min, under the present condition, whereas the parent carba-LNA AON (AON **2**) and the modified carba-LNA containing AONs show improved 3′-exonuclease resistance to a variable extent. Because the AONs were modified at position ***T***13, the phosphate P14 (see the structure in Figure 4 for phosphate (P) numbering) has considerably improved stability toward 3′-exonuclease. ***T***13 modification can also improve the stability of the phosphate P13 to some extent, which was also observed in the previous study,[19] and hence two bands corresponding to 14mer and 13mer could be observed on the PAGE pictures (Figure 3). However, once the P13 cleaved, AON was degraded to the monomer blocks quickly, and thus no bands corresponding to 12mer to dimer oligos could be observed.

Total percentages of integrated 14mer and 13mer AONs were plotted against time points to give SVPDE digestion curves for each AON in Figure 4, and pseudo-first-order reaction rates could be obtained by fitting the curves to single-exponential decay functions. A comparison of digestion rates of AONs with different types of modifications showed the following results:

(1) Parent unsubstituted carba-LNA incorporated AON (AON **2**) (k = 1.0473 ± 0.0601 h^{-1}) has greatly improved resistance to degradation compared to LNA incorporated AON (AON **22**) (k = 52.5135 ± 1.0968 h^{-1}), which has stability similar to that of the native AON (AON **1**).

(2) All substituted carba-LNA incorporated AONs (AON **6**, **10**, **14**, **18**, **26**, **30**, **34**) show higher stability toward 3′-exonuclease compared to that of the parent carba-LNA

(49) Shaw, J. P.; Kent, K.; Bird, J.; Fishback, J.; Froehler, B. *Nucleic Acids Res.* **1991**, *19*, 747–750.

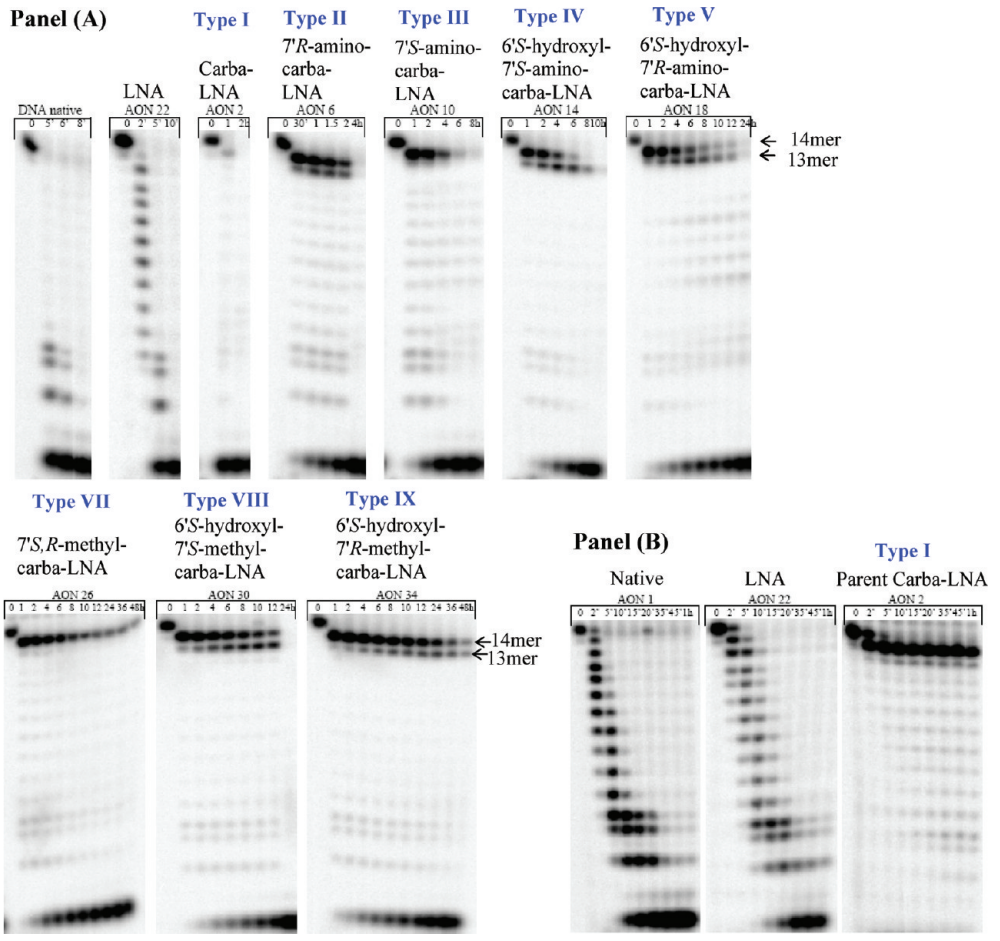

FIGURE 3. Denaturing PAGE analysis of the SVPDE degradation of AONs with functionalized carba-LNA modifications. Digestion conditions: AON 3 μM (5′-end ^{32}P-labeled with specific activity 80,000 cpm), 100 mM Tris-HCl (pH 8.0), 15 mM $MgCl_2$, reaction temperature 21 °C, total reaction volume 30 μL. (A) Higher concentration (6.7 ng/μL) of SVPDE was used. (B) Lower concentration (2.2 ng/μL) of SVPDE was used.

incorporated AON (AON **2**), suggesting that the substituents at 6′ and 7′ could perturb the interaction between nuclease and phosphate linkage and hence stabilize the AONs.

(3) By comparing the degradation kinetics of 7′*R* or *S*-amino-carba-LNA (Type II and Type III) modified AON **6** and **10** (k = 0.2820 ± 0.0298 and 0.2768 ± 0.0082 h^{-1}, respectively) with 7′-methyl-carba-LNA (Type VII) modified AON **26** (k = 0.1343 ± 0.0052 h^{-1}), 6′*S*-hydroxyl-7′-amino-carba-LNA (Type IV and Type V) modified AON **14** and **18** (k = 0.1047 ± 0.0046 and 0.1050 ± 0.0087 h^{-1}, respectively) with 6′*S*-hydroxyl-7′-methyl-carba-LNA (Type VIII and Type IX) modified AON **30** and **34** (k = 0.0563 ± 0.0040 and 0.0447 ± 0.0019 h^{-1}, respectively), it can be concluded that the hydrophobic methyl substitution at 7′ had more positive effects on the enzymatic stability of the modified carba-LNA containing AONs compared to that of the hydrophilic amino group, although they both stabilize the modified carba-LNA containing AONs more compared to the parent unsubstituted carba-LNA containing AON (AON **2**) (k = 1.0473 ± 0.0601 h^{-1}).

(4) 6′*S*-Hydroxyl-7′*S*-amino-carba-LNA (Type IV) modified AON **14** (k = 0.1047 ± 0.0046 h^{-1}) and 6′*S*-hydroxyl-7′*R*-amino-carba-LNA (Type V) modified AON **18** (k = 0.1050 ± 0.0087 h^{-1}) were two times more stable than 7′*R*-amino-carba-LNA (Type II) modified AON **6** (k = 0.2820 ± 0.0298 h^{-1}) and 7′*S*-amino-carba-LNA (Type III) modified AON **10** (k = 0.2768 ± 0.0082 h^{-1}), respectively, suggesting that the introduction of the 6′*S*-hydroxyl can improve the resistance to 3′-exonuclease of AONs. The bands corresponding to 13mer in the PAGE pictures of AON **14** and AON **18** disappeared relatively more slowly than those in the PAGE pictures of AON **6** and AON **10**, respectively (Figure 3A), suggesting that the introduction of 6′*S*-hydroxyl stabilize the AONs mainly by improving the nuclease resistance of 5′-phosphate (P13 in Figure 4) ($d_{C6'S\text{-hydroxyl-}5'P}$ ≈ 4.6 Å), which was also observed in the previous study.[19]

10.1. Role of Configuration of the 7′-Amino (*S* versus *R*) Group in Carba-LNAs in the Modulation of Stability toward 3′-Exonuclease. There were only slight difference in the enzymatic stability between 7′*R*-amino-carba-LNA (Type II) modified AON **6** and 7′*S*-amino-carba-LNA (Type III) modified AON **10**, 6′*S*-hydroxyl-7′*S*-amino-carba-LNA (Type IV) modified AON **14** and 6′*S*-hydroxyl-7′*R*-amino-carba-LNA (Type V) modified AON **18** in the digestion rates of AONs obtained in Figure 4, which seemed to suggest that the orientation of 7′-amino only had a small effect on the stability toward 3′-exonuclease of AONs.

However, the role of configuration of the 7′-amino in the modulation of nuclease stability could be observed on the PAGE gel pictures in which the bands corresponding to

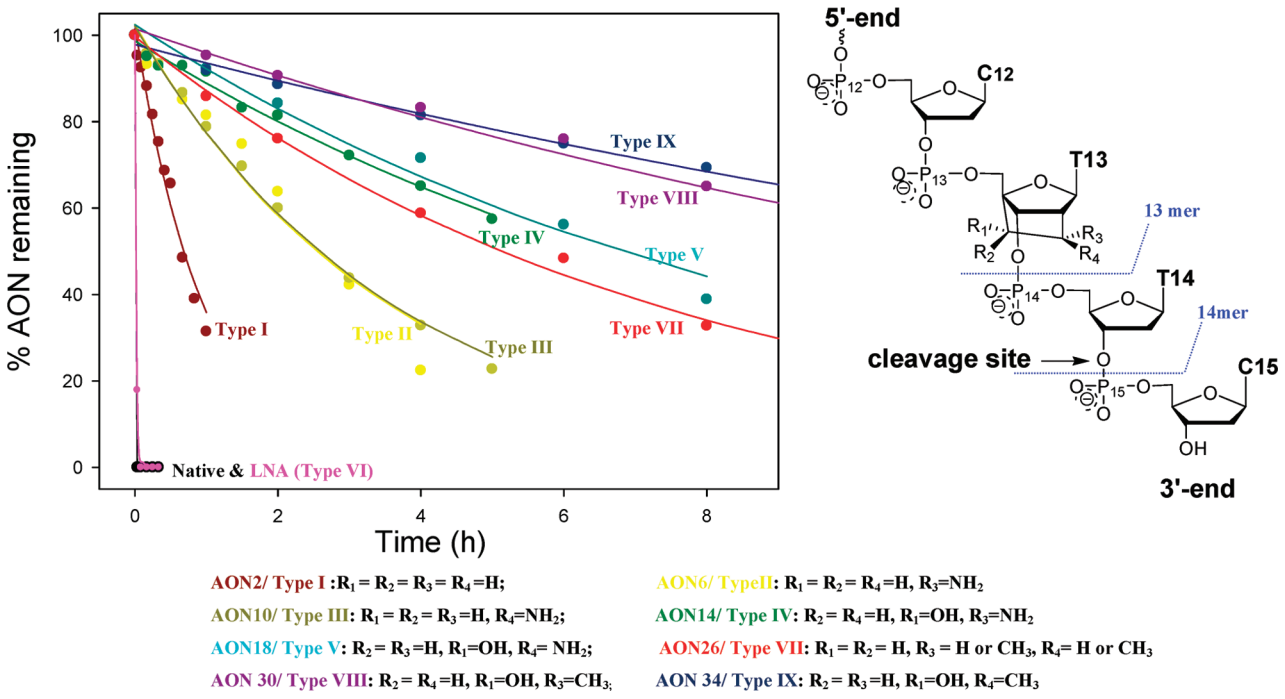

FIGURE 4. Amount of remaining initial oligonucleotide (taken 14mer and 13mer together in the calculation of percent remaining) during 3′-exonuclease (SVPDE)-promoted digestion. Following digestion condition was used: AON 3 μM (5′-end ^{32}P-labeled with specific activity 80000 cpm), 100 mM Tris-HCl (pH 8.0), 15 mM $MgCl_2$, SVPDE 6.7 ng/μL, reaction temperature 21 °C, total reaction volume 30 μL. Molecular structure of *T*13 modified AON with carba-LNA is also shown in the figure.

14mer in the PAGE pictures (Figure 3A) of AONs **10** and **18** (with the 7′-amino pointing at the 3′-phosphate) disappeared relatively more slowly than those in the PAGE pictures of AONs **6** and **14** (with the 7′-amino pointing away from the 3′-phosphate), respectively, whereas the bands corresponding to 13mer in the gel pictures of AONs **10** and **18** disappeared relatively more rapidly than those found in the PAGE pictures of AONs **6** and **14**, respectively, suggesting that the amino group can improve nuclease resistance of 3′-phosphate of AONs when it is pointed at the 3′-phosphate ($d_{C7'amino(up)\text{-}3'P} \approx 4.2$ Å). In contrast, when 7′-amino group is pointed at the 5′-phosphate ($d_{C7'amino(down)\text{-}5'P} \approx 6.8$ Å) it can stabilize the 5′-phosphate. So, the overall effects of two opposite orientations of the 7′-amino group on the 3′-phosphate and 5′-phosphate were very similar, leading to the similar degradation kinetic patterns in Figure 4 because products formed from the cleavage at P14 and P13 were considered together for rate calculation.

To confirm the role of 7′-amino stereochemistry in the modified carba-LNAs, we have estimated the relative rates of cleavage at P14 only (taking only the percentage of integrated 14mer AONs formed) for each AON (see Figure SII.22 in Supporting Information). This shows that when the 7′-amino is pointing away from the 3′-phosphate [as in 7′*R*-amino-carba-LNA (Type II) modified AON **6** ($k = 0.4304 \pm 0.0308$ h^{-1}) and 6′*S*-hydroxyl-7′*S*-amino-carba-LNA (Type IV) modified AON **14** ($k = 0.2709 \pm 0.0097$ h^{-1})], the corresponding AONs showed higher digestion rates compared to the AONs with 7′-amino pointing at the 3′-phosphate [as in 7′*S*-amino-carba-LNA (Type III) modified AON **10** ($k = 0.2781 \pm 0.0084$ h^{-1}) and 6′*S*-hydroxyl-7′*R*-amino-carba-LNA (Type V) modified AON **18** ($k = 0.2095 \pm 0.0153$ h^{-1})], respectively.

These results, taken together, suggested that as the scissile phosphate came closer to the hydrophilic and positively charged 7′-amino substituent, it became more stable toward the nuclease degradation. The improved nuclease resistance conferred by the hydrophilic and positively charged nature of the amino group could be plausibly explained by the fact that the amino group at 7′ could become a zwitterionic form at the physiological pH, and such zwitterionic AONs may escape exonuclease degration by displacing a catalytically important metal ion from the active site,[8] which was also observed by Griffey's group recently by synthesizing and analyzing 2′-*O*-aminopropyl ribonucleotides.[6]

10.2. Comparison of Nuclease Resistance of the Parent Unsubstituted Carba-LNA versus 2′-Oxa-LNA (LNA). Although the parent unsubstituted carba-LNA incorporated AON (AON **2**) was nucleolytically less stable than the other substituted carba-LNA incorporated AONs (AONs **6**, **10**, **14**, **18**, **26**, **30**, **34**), it would however give more accurate impression on the consequence of substitution of 2′-oxa in LNA with 2′-CH_2 in the isosteric carba-LNA and rule out any additional modulation effect conferred by the substituents at the 2′,4′-linkage of carba-LNA, when the nucleolytic stability of the parent carba-LNA incorporated AON is directly pairwise compared with the isosequential 2′-oxa-LNA (LNA) counterpart.[9,10] In the above experiment (with the high concentration of SVPDE in Figure 3A), the parent carba-LNA incorporated AON (AON **2**) and LNA incorporated AON (AON **22**) were degraded so fast that only an approximate degradation rate could be obtained. To give more accurate degradation kinetics, AON **2** and **22** were incubated with a lower concentration of SVPDE [SVPDE 2.2 ng/μL, AON 3 μM, 100 mM Tris-HCl (pH 8.0), 15 mM $MgCl_2$, 21 °C, total volume 30 μL] compared to the native

TABLE 2. Degradation Rates k_1 (h^{-1}) for All Modified Carba-LNAs and Carba-ENAs[a]

Modification Type	R_1	R_2	R_3	R_4	n	Degradation Rate k_1 (h^{-1})
Type I	H	H	H	H	0	**1.0473 ± 0.0601 h^{-1}**
Type II	H	H	NH_2	H	0	**0.2820 ± 0.0298 h^{-1}**
Type III	H	H	H	NH_2	0	**0.2768 ± 0.0082 h^{-1}**
Type IV	OH	H	NH_2	H	0	**0.1047 ± 0.0046h^{-1}**
Type V	OH	H	H	NH_2	0	**0.1050 ± 0.0087 h^{-1}**
Type VII	H	H	H or CH_3	H or CH_3	0	**0.1343 ± 0.0052 h^{-1}**
Type VIII	OH	H	CH_3	H	0	**0.0563 ± 0.0040 h^{-1}**
Type IX	OH	H	H	CH_3	0	**0.0447 ± 0.0019 h^{-1}**
Type X	H	OH	CH_3	H	0	**10.4896 ± 1.2408 h^{-1}**
Type XI	H	OH	H	CH_3	0	**1.8568 ± 0.2288 h^{-1}**
Type XII	H or CH_3	H or CH_3	CH_3	H	0	**0.0192 ± 0.0011 h^{-1}**
Type XIII	OH	CH_3	CH_3	H	0	**0.0801 ± 0.0044 h^{-1}**
Type XV	H	H	CH_3	H	1	**0.1008 ± 0.0026 h^{-1}**
Type XVI	OH	H	CH_3	H	1	**0.1865 ± 0.0084 h^{-1}**
Type XVII	H	OH	CH_3	H	1	**0.5897 ± 0.0384 h^{-1}**
Type XVIII	CH_3	H	CH_3	H	1	**0.0351 ± 0.0018 h^{-1}**
Type XIX	H	CH_3	CH_3	H	1	**0.0342 ± 0.0012 h^{-1}**

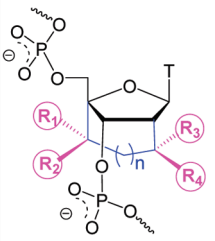

[a]The degradation rates k (h^{-1}) value was calibrilated for Types X−XIX, published in our previous study,[19] by using the correlation coefficient obtained from dividing the observed value (k_1) in the present study for Type VII by the observed value (k_2) for Type VII in the earlier study, which has been used to calibrate other k_2 values.

AON (AON **1**). The gel pictures obtained by autoradiography are shown in Figure 3B and the degradation curves are shown in Figure SII.21 in Supporting Information. Under this condition, the parent carba-LNA incorporated AON (AON **2**) ($k = 0.0015 \pm 0.0002$ h^{-1}) was found to be 145 times more stable than LNA incorporated AON (AON **22**) ($k = 0.2195 \pm 0.0383$ h^{-1}), which on the other hand has degradation kinetics very similar to that of the native AON (AON **1**) ($k = 0.7617 \pm 0.0368$ h^{-1}). This result simply showed in a straightforward manner that the lipophilic 2′-CH_2- in the parent carba-LNA (compared to LNA) can indeed improve the nuclease resistance of the vicinal 3′-phosphate probably by decreasing the magnitude of hydration around it ($d_{C2'methylene\text{-}3'P} \approx 4.2$ Å).

10.3. Structure−Activity Relationships of All Modified Carba-LNAs and Carba-ENAs for Nuclease Stability. From the observations on the structure−activity relationships of all modified carba-LNAs and carba-ENAs for nuclease stability (Table 2), the following summary may be made: (1) The methyl substitution can always improve nuclease resistance of AONs, independent of its location and configuration on the 2′,4′-carba bridge. The improved nuclease resistance conferred by the lipophilic nature of the methyl group could be explained by two effects: First, the methyl group counld decrease the extent of hydration around the vincinal phosphate ($d_{C7'methyl(up)\text{-}3'P} \approx 4.3$ Å, $d_{C6'methyl(down)\text{-}5'P} \approx 4.6$ Å). Second, the bulky methyl could also interfere with the interaction between nuclease and phosphate linkage by the steric clash effect which was also observed by Imanishi's group.[20] (2) The amino substitution at C7′ can also improve the stability of AONs regardless of its orientation ($k = 0.2820 \pm 0.0298$ h^{-1} for Type II versus $k = 0.2768 \pm 0.0082$ h^{-1} for Type III) but in a less pronounced way compared to the methyl group ($k = 0.1343 \pm 0.0052$ h^{-1} for Type VII), suggesting that the steric effect conferred by the substituents is more important than the electrostatic effect on the stability toward nuclease. (3) The role of hydrophilic modification with a hydroxyl group at the C6′ position is more complex. The opposite orientation of 6′-hydroxyl group (*S* versus *R*) can lead to a completely opposite effect on the stability of AONs and hence should be handled very carefully. The C6′-hydroxyl pointing at 5′-phosphate ($d_{C6'hydroxyl(down)\text{-}5'P} \approx 4.6$ Å) can stabilize the proximate 5′-phosphate ($k = 0.0563 \pm 0.0040$ h^{-1} for Type VIII and $k = 0.0447 \pm 0.0019$ h^{-1} for Type IX), whereas the C6′-hydroxyl pointing at 3′-phosphate ($d_{C6'hydroxyl(up)\text{-}3'P} \approx 4.5$ Å) makes the phosphate too labile toward the nuclease ($k = 10.4896 \pm 1.2408$ h^{-1} for Type X and $k = 1.8568 \pm 0.2288$ h^{-1} for Type XI). How the C6′-hydroxyl interfere with the modulation of the stability of AONs is still very poorly understood. (See SII.34−35 in Supporting Information for detailed pairwise comparison.)

11.0. Lessons from the Target Affinity vis-à-vis Nuclease Resistance for the Design of AONs. Combining the target affinity with nuclease resistance of modified AONs, the

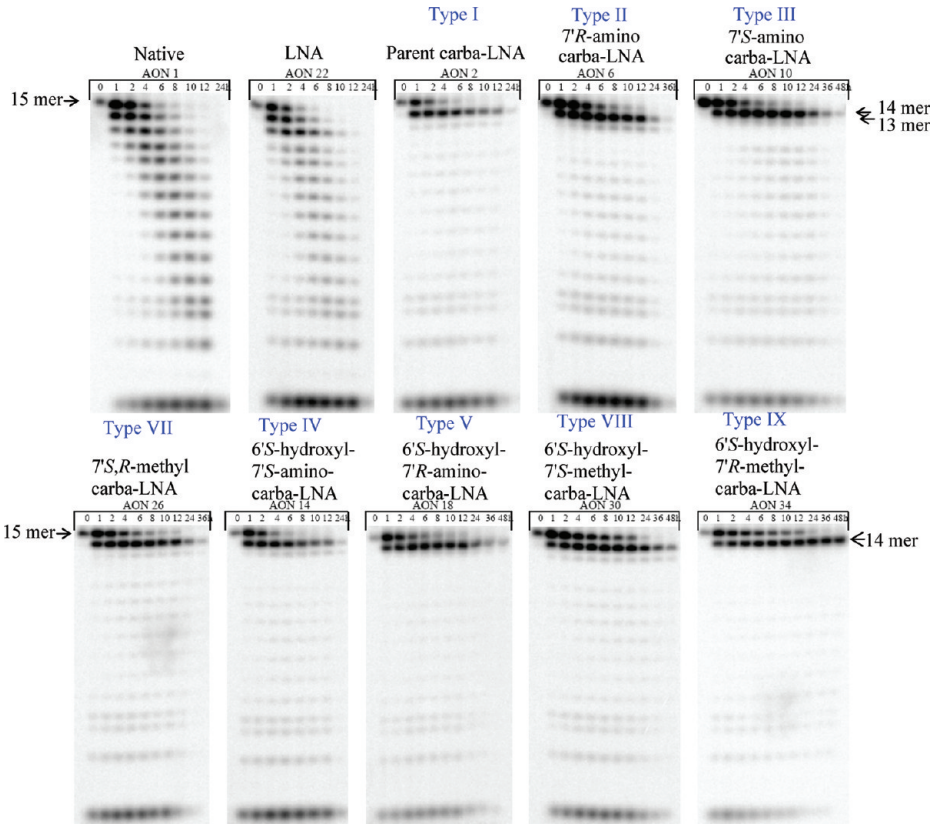

FIGURE 5. Autoradiograms of 20% denatured PAGE showing the stability of 5′-^{32}P-labeled AONs in human blood serum in the present study.

following conclusions can be drawn: (1) In the center of the minor groove, both hydrophobic methyl substitution and hydrophilic amino substitution are not favored, which causes loss of target affinity toward RNA. (2) At the border of minor grooves, the hydrophobic methyl group and the hydrophilic 6*S*′-hydroxyl (pointing away from 3′-phosphate) can improve the enzymatic stability without loss of target affinity toward RNA and hence are proposed as suitable candidates for future modification in the AONs. (3) The hydrophilic 6*R*′-hydroxyl (pointing at 3′-phosphate) renders the modified AONs the most susceptible to enzymatic degradation, and hence this modification should be avoided.

12.0. Stability of Parent Carba-LNA and Modified Carba-LNA AONs in the Human Blood Serum. Blood serum stabilities of all newly synthesized AONs modified at the third position (position ***T***13) from the 3′-end (AONs **2**, **6**, **10**, **14**, **18**) and the known AON counterparts (AON **22**, **26**, **30**, **34**) with a single modification at position ***T***13 (Table 1) have also been tested in the present studies. The AONs (^{32}P-labeled at 5′-end) were incubated with human blood serum (male, type AB) for up to 48 h at 21 °C, and aliquots were taken out at regular time intervals and analyzed by 20% denaturing PAGE. The gel pictures obtained by autoradiography are shown in Figure 5. [Caution: Although it was seriously attempted to carry out the experiment under the same condiction as the previous study,[19] the enzymatic activity of the blood serum may vary from batch to batch and from donor to donor. So the result obtained in the present study should/could not be used for direct parallel comparison with the previous result.[19] This study of blood serum stability should be treated as an independent study and can only be compared within the present candidates]. Although the quantified data from the gel picture could not be obtained because the alkaline phosphatase in serum removed the 5′-end ^{32}P-label gradually, it could be seen by visualization of the gel that the parent carba-LNA incorporated AON (AON **2**) (the bands corresponding to 14mer of parent carba-LNA containing AON **2** in the gel pictures persisted up to 12 h under the present condition) was more stable than LNA incorporated AON (AON **22**) and native AON (AON **1**), both of which were however degraded completely within 8 h. All the substituted carba-LNA modified AONs in present study (AON **6**, **10**, **14**, **18**, **26**, **30**, **34**) were more stable than the parent carba-LNA incorporated AON (AON **2**) in which the 6′*S*-hydroxyl-7′-methyl carba-LNA AONs (AON **30**, **34**) were more stable than 6′*S*-hydroxyl-7′-amino substituted carba-LNA containing AONs (AON **14**, **18**) with the same configuration at C6′ and C7′, suggesting that the methyl group has a more positive effect on stability of AONs than that of the amino group in human blood serum. However, the extra stabilization conferred by the 6′*S*-hydroxyl, which was observed upon treatment with 3′-exonuclease, was not marked in the stability assay in the blood serum when comparing AON **6** with AON **14** and AON **10** with AON **18** in Figure 5. So, in summary, the relative stabilities in blood serum for all modified carba-LNA in present study is as followings: AON **34** (Type IX) > AON **30** (Type VIII) > AON **18** (Type V) > AON **10** (Type III) > AON **26** (Type VII) ≈

AON **6** (Type II) > AON **2** (Type I) ≈ AON **14** (Type IV) > AON **22** (LNA) ≈ AON **1** (native). The effects on the stability in human blood serum imparted by the substituent at 2′,4′-connection follow the similar trend as those observed upon treatment of 3′-exonuclease.

FIGURE 6. *Escherichia coli* RNase H1 promoted cleavage pattern of AONs **1**−**29**/RNA duplexes. Vertical arrows show the RNase H cleavage sites, with the relative length of the arrow indicating the extent of the cleavage. The square boxes show the stretch of the modification, which is resistant to RNase H1 cleavage, thereby giving footprints.

13.0. RNase H Digestion Study of Carba-LNA Modified AON/RNA Duplexes. The RNase H recruitment capabilities of a series of four 7′-amino-carba-LNA substituted AONs (Types II−V) and parent carba-LNA substituted AONs (Type I) were studied, using native AON (AON **1**) as a reference, whereas Type VI containing AONs (LNA) and Type VII containing AONs (7′-methyl-carba-LNA) were used in a parallel experiment for comparison. The gel pictures obtained are shown in Figure SII.23, from which we can see that all modified AONs **2**−**29** in the corresponding AON/RNA duplexes were good substrates for RNase H, and the cleavage patterns were all very similar, independent of the nature of the modification, but were dependent on the site of modification within the AON. Just as in the previous study,[18,19] the cleavage activity of RNase H was suppressed within a 5−6 base pairs long region that starts from the base opposite to the modified ***T*** nucleotide in AON/RNA duplex toward the 3′-end of the RNA strand. However, the preferred cleavage site shifts to the edges of the suppressed region as is shown in Figure 6. Hence, the overall RNase recruitment capabilities were not impared significantly compared to native AON **1**/ RNA duplex, as is shown in Figure 7. The cleavage rates of parent carba-LNA modified AONs/RNA and 7′-amino-carba-LNA modified AONs/RNA are even increased compared to native one, in which the AON **10**/RNA (Type III) has three times cleavage rate as that of native AON **1**/RNA. (For detailed discussion see SII.36 in Supporting Information).

Conclusions

The first syntheses of the parent fully unsubstituted carba-LNA and its C7′-amino substituted and/or C6′-hydroxyl substituted derivatives were accomplished by using an intramolecular 5-*exo* free-radical addition to a C=N double bond of the appropriately protected oxime-ether. Various NMR experiments, including ^{1}H, ^{13}C, DEPT, one bond ^{1}H−^{13}C correlation (HMQC) and long-range ^{1}H−^{13}C

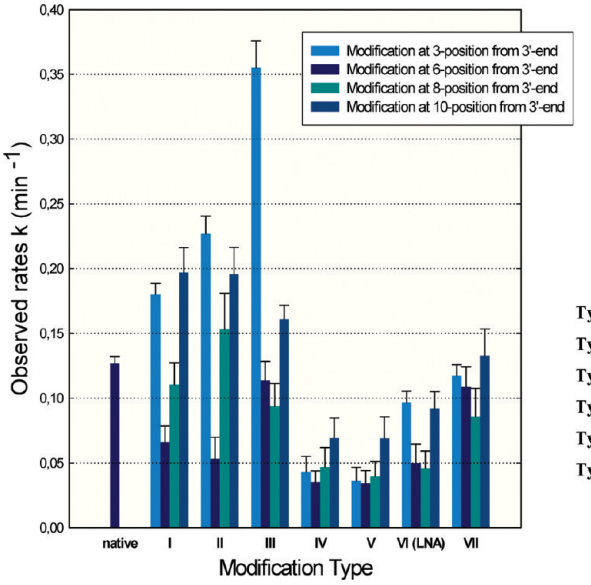

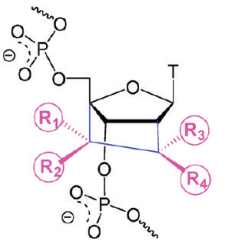

Type I : $R_1 = R_2 = R_3 = R_4 = H$;
TypeII: $R_1 = R_2 = R_4 = H$, $R_3 = NH_2$
Type III: $R_1 = R_2 = R_3 = H$, $R_4 = NH_2$;
Type IV: $R_2 = R_4 = H$, $R_1 = OH$, $R_3 = NH_2$
Type V: $R_2 = R_3 = H$, $R_1 = OH$, $R_4 = NH_2$;
Type VII: $R_1 = R_2 = H$, $R_3 = H$ or CH_3, $R_4 = H$ or CH_3

FIGURE 7. Bar plots of the observed cleavage rates of the RNase H1 promoted degradation of RNA in AON **1**−**29**/RNA hybrid duplexes.

HMBC, have been employed to characterize all synthesized compounds. The configuration of subsituents in the key intermediates was determined by NOE and was also corroborated by the $^3J_{H,H}$ coupling constants obtained from ^{1}H homodecoupling experiments.

The corresponding phosphoramidites **21a/b**, **24**, **31a/b** were incorporated as mono substitution in a 15mer DNA sequence on an automated RNA/DNA synthesizer. The investigation for the antisense properties of resulting AONs reveals that the substitution and its orientation at C6′ and C7′ play an important role in the modulation of modified carba-LNA. The relationship between substitution and target affinity and nuclease resistance of AONs can be summarized as follows: (i) The hydrophobic methyl group and the hydrophilic amino group at 7′ both can impair the thermal stability of AON/RNA duplex to a similar extent especially when the substituents point at the vicinal 3′-phosphate. (ii) In contrast, substitution at C7′ with either CH_3 or NH_2 can stabilize the carba-LNA modified AONs compared to the parent carba-LNA modified AON. The CH_3 substitution at C7′ gives more pronounced positive effects on stabilities of modified AONs. The orientation of substituents (CH_3 or NH_2) plays a very important role for the selective stabilization for the 3′-phosphate versus 5′-phophate in the exonuclease cleavage reaction. (iii) The introduction of 6′*S*-hydroxyl can not only improve the thermal affinity toward the complementary RNA of the corresponding AONs but also stabilize the AONs against 3′-exonuclease and hence is recommended as a suitable modification for carba-LNAs.

For the RNase H mediated RNA cleavage in the AON/RNA hybrid, the cleavage pattern was not affected by the nature of different substituents but depended upon the site of the modification. The RNase H has strong positional preference for a given active DNA/RNA hybrid. As for the cleavage rate by RNase H, the parent carba-LNAs and 7′-amino carba-LNAs show improved recruitment capabilities compared to LNAs and native AON, in which the heteroduplex with 7′*S*-amino carba-LNAs (Type III) has the fastest cleavage rate (AON **10**/RNA has three times cleavage rate as that of native AON **1**/RNA).

Experimental Section

Note. The individual characterization for all intermediates are given in Supporting Information (Part I). All individual reaction steps, workup, and product characterization for the intermediates in Scheme 3 and the characterization for final amidites **21a,b**, **24**, and **31a,b** are given in Supporting Information (SII.37−46)

1-(2-Hydroxyl-3,5-di-*O*-benzyl-4-*C*-cyanomethyl-β-D-ribofuranosyl)-thymine (16). Compound **10** (6.87 g, 13.2 mmol) was dissolved in methanol (30 mL) and methylamine solution (210 mL). The mixture was stirred at rt for 1 h. After evaporation of the solvent, the residue was purified by column chromatography on silica gel (1% methanol in CH_2Cl_2, v/v) to obtain **16** (6 g, 95%) as white foam. ^{1}H NMR (500 MHz, $CDCl_3$): δ 10.6 (1H, broad, N*H*), 7.55 (1H, s, H6), 7.55−7.29 (10H, m, aromatic), 5.93 (1H, d, $J_{1',2'}$ = 4 Hz, H1′), 4.93 (1H, d, J_{gem} = 11 Hz, CH_2-Bn), 4.85 (1H, broad, O*H*), 4.66−4.55 (4H, m, CH_2Bn and H2′), 4.38 (1H, d, $J_{2',3'}$ = 5.5 Hz, H3′), 3.87 (1H, d, J_{gem} = 10 Hz, H5′), 3.62 (1H, d, J_{gem} = 10 Hz, H5″), 2.94 (1H, d, J_{gem} = 17.5 Hz, H6′), 2.62 (1H, d, J_{gem} = 17.5 Hz, H6″), 1.47 (3H, s, T-CH_3). ^{13}C NMR (125 MHz, $CDCl_3$): δ 162.6 (C4), 150.4 (C2), 136.5, 136.2 (aromatic), 134.8 (C6), 127.7, 127.5, 127.2, 127.0 (aromatic), 116.0 (*C*N), 110.0 (C5), 89.5 (C1′), 83.8 (C4′), 75.8 (C3′), 73.5 (*C*H_2Bn), 73.0 (*C*H_2Bn), 72.8 (C2′), 70.8 (C5′), 21.6 (C6′), 11.1 (T-*C*H_3). MALDI-TOF *m/z*: $[M + H]^+$, found 478.200, calcd 478.198.

4′-(Benzyloxyimino)ethyl-2′-hydroxyl-3′,5′-di-*O*-benzyl-thymidine (17). To a solution of **16** (6 g, 12.56 mmol) in dry dichloromethane (DCM, 130 mL) was added DIBALH (38 mL, 1.0 M solution in toluene) dropwise at −78 °C. After stirring at the same temperature for 4 h, the mixture was allowed to warm to 0 °C, and then 1 N HCl solution was added to quench the reaction and stirred for 30 min at 0 °C. The resulting suspension was diluted with DCM. The organic layer was separated and washed with brine, dried over $MgSO_4$, and coevaporated with dry pyridine twice to give crude compound **9**, which was dissolved in dry DCM (310 mL) and dry pyridine (6 mL). To this solution, *O*-benzyl hydroxylamine hydrochloride (5 g, 31.4 mmmol) was added. After heating at reflux for 2 h, the mixture was cooled to rt and neutralized by the addition of saturated aqueous solution of $NaHCO_3$. The organic layer was separated, dried over $MgSO_4$, evaporated, and chromatographed over silica gel (0.5−1% methanol in DCM) to give **17** as the mixture of *Z* and *E* isomers (4.4 g, 7.53 mmol, 60% in two steps from **16**). ^{1}H NMR (500 MHz, $CDCl_3$): δ 9.10 (1H, broad, N*H*), 7.42 (0.5H, dd, $J_{7',6''}$ = 7.5 Hz, $J_{7',6'}$ = 5 Hz, H7′), 7.35 (1H, s, H6), 7.30−7.16 (15H, m, aromatic), 6.78 (0.5H, dd, $J_{7',6''}$ = 6 Hz, $J_{7',6'}$ = 5 Hz, H7′), 5.89 (1H, 2xd, $J_{1',2'}$ = 3.5 Hz, H1′), 5.02, 4.97(2H, 2xs, NOCH_2Bn), 4.69−4.34 (4H, m, CH_2Bn), 4.32 (1H, m, H2′), 4.08 (1H, 2xd, $J_{2',3'}$ = 2 Hz, H3′), 3.55−3.31 (3H, m, H5′,OH), 2.81 (0.5H, dd, J_{gem} = 15 Hz, $J_{6',7'}$ = 5 Hz, H6′), 2.72 (1H, m, H6″,H6′), 2.43 (0.5H, dd, J_{gem} = 15 Hz, $J_{7',6''}$ = 7.5 Hz, H6″), 1.50 (3H, s, T-CH_3). ^{13}C NMR (125 MHz, $CDCl_3$): δ 162.6 (C4), 149.9 (C2), 146.8 (C7′), 146.3 (C7′), 136.8, 136.1 (aromatic), 134.8 (C6), 127.7, 127.6, 127.1, 126.6 (aromatic), 110.1 (C5), 88.0 (C1′), 87.9 (C1′), 85.4 (C4′), 85.2 (C4′), 78.2 (C3′), 74.9 (*C*H_2Bn), 74.6 (*C*H_2Bn), 74.0 (C2′), 73.9 (C2′), 73.6 (*C*H_2Bn), 72.7 (*C*H_2Bn), 72.6 (C5′), 32.3 (C6′), 28.7 (C6′), 11.0 (T-*C*H_3). MALDI-TOF: *m/z*: $[M + H]^+$, found 586.248, calcd. 586.255.

4′-(Benzyloxyimino)ethyl-3′,5′-Di-*O*-benzyl-2′-*O*-phenoxythiocarbonyl-thymidine (18). To a solution of **17** (4.4 g, 7.73 mmol) in dry pyridine (150 mL) was added phenyl chlorothionoformate (1.34 mL, 10 mmol) dropwise at 0 °C. After stirring at rt for 2 h, saturated aqueous solution of $NaHCO_3$ was added, and the resulting mixture was extracted with DCM three times. The organic solvent was washed with water, then brine, dried over $MgSO_4$ and evaporated. The residue was chromatographed over silica gel (5−20% ethyl acetate in cyclohexane) to give **18** as *Z* and *E* isomers (4.2 g, 5.8 mmol, 75%). Isomer I: ^{1}H NMR (500 MHz, $CDCl_3$): δ 8.70 (1H, broad, N*H*), 7.52 (1H, app t, *J* = 6 Hz, H7′), 7.46 (1H, s, H6), 7.42−7.29 (18H, m, aromatic), 7.03 (2H, d, *J* = 8 Hz, aromatic), 6.42 (1H, d, $J_{1',2'}$ = 6.5 Hz, H1′), 6.03 (1H, app t, *J* = 5 Hz, H2′), 5.09 (2H, s, NOCH_2Bn), 4.74 (1H, d, J_{gem} = 11 Hz, CH_2Bn), 4.58 (1H, d, $J_{2',3'}$ = 5.5 Hz, H3′), 4.54 (2H, s, CH_2Bn), 4.50 (1H, d, J_{gem} = 11 Hz, CH_2Bn), 3.64 (1H, d, J_{gem} = 10 Hz, H5′), 3.58 (1H, d, J_{gem} = 10 Hz, H5″), 2.75 (1H, dd, $J_{6',7'}$ = 4.5 Hz, J_{gem} = 15 Hz, H6′), 2.56 (1H, dd, $J_{6'',7'}$ = 7.5 Hz, J_{gem} = 15 Hz, H6″), 1.56 (3H, s, T-CH_3). ^{13}C NMR (125 MHz, $CDCl_3$): δ 193.4 (C═S), 162.5 (C4), 152.4 (C2), 149.3 (aromatic), 146.4 (C7′), 136.7, 136.0 (aromatic), 134.8 (C6), 128.6, 127.6, 125.8, 120.6 (aromatic), 110.6 (C5), 85.9 (C4′), 84.6 (C1′), 81.7 (C2′), 76.8 (C3′), 74.6 (*C*H_2Bn), 73.9 (*C*H_2Bn), 72.8 (*C*H_2Bn), 72.7 (C5′), 32.2 (C6′), 11.0 (T-*C*H_3). MALDI-TOF *m/z*: $[M + H]^+$, found 722.20, calcd 722.25. Isomer II: ^{1}H NMR (500 MHz, $CDCl_3$): δ 8.70 (1H, broad, N*H*), 7.42−7.25 (19H, m, aromatic and H6), 7.00 (2H, d, *J* = 8 Hz, aromatic), 6.85 (1H, app t, *J* = 5 Hz, H7′), 6.37 (1H, d, $J_{1',2'}$ = 5.5 Hz, H1′), 5.96 (1H, app t, *J* = 5.5 Hz, H2′), 5.11 (2H, s, NOCH_2Bn), 4.75 (1H, d, J_{gem} = 11.5 Hz, CH_2Bn), 4.58 (2H, m, CH_2Bn, H3′), 4.46 (2H, s,

CH_2Bn), 3.62 (1H, d, J_{gem} = 10.5 Hz, H5′), 3.42 (1H, d, J_{gem} = 10.5 Hz, H5″), 2.86 (1H, dd, $J_{6',7'}$ = 4.5 Hz, J_{gem} = 16 Hz, H6′), 2.76 (1H, dd, $J_{6'',7'}$ = 6 Hz, J_{gem} = 16 Hz, H6″), 1.52 (3H, s, T-CH_3). ^{13}C NMR (125 MHz, $CDCl_3$): δ 193.4(C=S), 162.5 (C4), 152.3 (aromatic), 149.9 (C2), 146.0 (C7′), 136.7, 136.0 (aromatic), 134.7 (C6), 128.6, 125.8, 120.6 (aromatic), 110.6 (C5), 85.8 (C4′), 85.0 (C1′), 81.6 (C2′), 77.7 (C3′), 75.0 (*C*H_2Bn), 74.0 (*C*H_2Bn), 72.7-(*C*H_2Bn), 71.6 (C5′), 28.6 (C6′), 11.0 (T-*C*H_3). MALDI-TOF *m*/*z*: $[M + H]^+$, found 722.28, calcd 722.25.

(1*R*,3*R*,4*R*,5*R*,7*S*)-7-Benzyloxy-1-benzyloxymethyl-5-benzyloxyamino-3-(thymin-1-yl)-2-oxa-bicyclo[2.2.1]heptane (2a) and (1*R*,3*R*,4*R*,5*S*,7*S*)-7-Benzyloxy-1- benzyloxymethyl-5-benzyloxyamino-3-(thymin-1-yl)-2-oxa-bicyclo[2.2.1]heptane (2b). Compound **18** (4 g, 5.5 mmol) was dissolved in dry toluene (545 mL), to which N_2 was purged for 40 min. The mixture was refluxed, and Bn_3SnH (2.7 mL in 40 mL dry toluene) and AIBN (210 mg in 20 mL dry toluene) were added very slowly in 7 h. After addition, the reflux was continued for 1 h. The solvent was evaporated, and the residue was applied to chromatography (5−20% ethyl acetate in cyclohexane) to give the two diastereomers **2a** (1.87 g, 60%) and **2b** (125 mg, 4%). **2a**: ^{1}H NMR (600 MHz, $CDCl_3$): δ 9.18 (1H, s, N*H*), 7.65 (1H, s, H6), 7.65−7.15 (15H, m, aromatic), 6.11 (1H, s, H1′), 5.54 (1H, broad, N*H*), 4.87 (1H, d, J_{gem} = 12 Hz, CH_2Bn), 4.78 (1H, d, J_{gem} = 12 Hz, CH_2Bn), 4.51 (1H, d, J_{gem} = 12 Hz, CH_2Bn), 4.47 (2H, d, J_{gem} = 12 Hz, CH_2Bn), 4.36 (1H, d, J_{gem} = 12 Hz, CH_2Bn), 4.03 (1H, s, H3′), 3.94 (1H, dt, $J_{2',7'}$ = 4.2 Hz, $J_{6',7'}$ = 10.2 Hz, $J_{6'',7'}$ = 4.2 Hz, H7′), 3.71 (1H, d, J_{gem} = 10.8 Hz, H5′), 3.60 (1H, d, J_{gem} = 10.8 Hz, H5″), 2.95 (1H, d, $J_{2',7'}$ = 4.2 Hz, H2′), 1.98 (1H, dd, J_{gem} = 12.6 Hz, $J_{6',7'}$ = 10.2 Hz, H6′), 1.49 (3H, s, T-CH_3), 1.12 (1H, dd, J_{gem} = 12.6 Hz, $J_{6'',7'}$ = 4.2 Hz, H6″). ^{13}C NMR (125 MHz, $CDCl_3$): δ 163.3 (C2), 149.0 (C4), 137.0, 136.7, 136.2 (aromatic), 135.4 (C6), 128.5, 127.7, 127.5, 127.4, 127.3, 127.2, 126.8, 126.5 (aromatic), 108.2 (C5), 86.7 (C4′), 82.8 (C1′), 77.6 (C3′), 75.3 (*C*H_2Bn), 72.7 (*C*H_2Bn), 71.0 (*C*H_2-Bn), 66.3 (C5′), 56.3 (C7′), 44.5 (C2′), 33.4 (C6′), 11.2 (T-*C*H_3). MALDI-TOF *m*/*z*: $[M + H]^+$, found 570.264, calcd 570.260. **2b**: ^{1}H NMR (600 MHz, $CDCl_3$): δ 8.45 (1H, broad, N*H*), 7.66 (1H, s, H6), 7.37−7.19 (15H, m, aromatic), 5.88 (1H, broad, N*H*), 5.37 (1H, s, H1′), 4.75 (1H, d, J_{gem} = 12 Hz, CH_2Bn), 4.71 (1H, d, J_{gem} = 12 Hz, CH_2Bn), 4.62−4.56 (3H, m, CH_2Bn), 4.46 (1H, d, J_{gem} = 12 Hz, CH_2Bn), 4.04 (1H, s, H3′), 3.84 (1H, d, J_{gem} = 10.8 Hz, H5′), 3.75 (1H, d, J_{gem} = 10.8 Hz, H5″), 3.69 (1H, m, H7′), 3.16 (1H, s, H2′), 2.05 (1H, dd, J_{gem} = 13.2 Hz, $J_{6'',7'}$ = 8.4 Hz, H6″), 1.58 (1H, dd, J_{gem} = 13.2 Hz, $J_{6',7'}$ = 4.0 Hz, H6′), 1.56 (3H, s, T-CH_3). ^{13}C NMR (125 MHz, $CDCl_3$): δ 162.8 (C4), 148.7 (C2), 137.1, 136.6, 135.7 (aromatic), 134.8 (C6), 127.6, 127.5, 127.3, 127.1, 126.8, 126.7 (aromatic), 108.2 (C5), 86.7 (C4′), 85.3 (C1′), 77.3 (C3′), 74.7 (*C*H_2Bn), 72.7 (*C*H_2Bn), 71.6 (*C*H_2Bn), 66.2 (C5′), 59.7 (C7′), 43.5 (C2′), 35.1 (C6′), 11.1 (T-*C*H_3). MALDI-TOF *m*/*z*: $[M + H]^+$, found 570.258, calcd 570.260.

(1*R*,3*R*,4*R*,5*R*,7*S*)-7-Benzyloxy-1-benzyloxymethyl-5-trifluoroacetoxyamino-3-(thymin-1-yl)-2-oxa-bicyclo[2.2.1]heptane (19a). To a solution of **2a** (300 mg, 0.53 mmol) in dry methanol (15 mL) were added 10% Pd/C (262 mg) and ammonium formate (661 mg, 10.48 mmol). After stirring at rt for 4 h, the mixture was filtered through a Celite pad, and the organic solvent was evaporated to dryness. The residue was dissolved in anhydrous methanol. Ethyl trifluoroacetate (0.63 mL, 5.3 mmol) and 4-dimethylamino-pyridine (DMAP, 130 mg, 1.06 mmol) were added, and the mixture was stirred at rt overnight. The solvent was removed and the residue was applied to chromatography (1−2% methanol in DCM) to give **19a** (148 mg, 50% in two steps). ^{1}H NMR (500 MHz, $CDCl_3$): δ 8.99 (1H, s, N*H*), 7.62 (1H, s, H6), 7.37−7.27 (11H, m, aromatic and N*H*), 5.92 (1H, s, H1′), 4.77 (1H, m, H7′), 4.64−4.50 (4H, m, CH_2Bn), 4.13 (1H, s, H3′), 3.85 (1H, d, J_{gem} = 11 Hz, H5′), 3.73 (1H, d, J_{gem} = 11 Hz, H5″), 3.04 (1H, s, H2′), 2.48 (1H, dd, J_{gem} = 13 Hz, $J_{6',7'}$ = 11 Hz, H6′), 1.58 (4H, m, H6″ and T-CH_3). ^{13}C NMR (125 MHz, $CDCl_3$): δ 163.9 (C4), 157.9 (q, *J* = 36 Hz, *C*OCF_3), 150.0 (C2), 137.5, 136.7 (aromatic), 135.5 (C6), 128.6, 128.3, 128.1, 127.8 (aromatic), 116.8, 114.5 (q, *J* = 286 Hz, *C*F_3), 110.1 (C5), 88.1 (C4′), 82.9 (C1′), 77.8 (C3′), 73.8 (*C*H_2Bn), 72.4 (*C*H_2Bn), 66.9 (C5′), 47.6 (C7′), 46.9 (C2′), 36.9 (C6′), 12.1 (T-*C*H_3). MALDI-TOF *m*/*z*: $[M + Na]^+$, found 582.181, calcd 582.183.

(1*R*,3*R*,4*R*,5*S*,7*S*)-7-Benzyloxy-1-benzyloxymethyl-5-trifluoroacetoxyamino-3-(thymin-1-yl)-2-oxa-bicyclo[2.2.1]heptane (19b). Compound **19b** (58 mg, 49% in two steps) was obtained from **2b** after following the same reaction and workup procedure as **19a**. ^{1}H NMR (500 MHz, $CDCl_3$): δ 8.41 (1H, s, N*H*), 7.64 (1H, s, H6), 7.38−7.33 (8H, m, aromatic), 7.21−7.19 (2H, m, aromatic), 7.06 (1H, d, $J_{NH,H7'}$ = 9.5 Hz, N*H*), 5.44 (1H, s, H1′), 4.67−4.56 (5H, m, H7′, CH_2Bn), 4.16 (1H, s, H3′), 3.89 (1H, d, J_{gem} = 11 Hz, H5′), 3.79 (1H, d, J_{gem} = 11 Hz, H5″), 2.71 (1H, s, H2′), 2.34 (1H, dd, J_{gem} = 14 Hz, $J_{6',7'}$ = 8.5 Hz, H6′), 1.72 (1H, dd, J_{gem} = 14 Hz, $J_{6'',7'}$ = 3.5 Hz, H6″), 1.61 (T-CH_3). ^{13}C NMR (125 MHz, $CDCl_3$): δ 162.5 (C4), 154.6 (q, *J* = 36 Hz, *C*OCF_3), 148.6 (C2), 136.2, 135.1 (aromatic), 134.2 (C6), 127.8, 127.7, 127.3, 126.9, 126.7 (aromatic), 115.8, 113.5(q, *J* = 286 Hz, *C*F_3), 108.7 (C5), 87.0 (C4′), 84.3 (C1′), 78.0 (C3′), 72.9 (*C*H_2Bn), 72.5 (*C*H_2Bn), 65.9 (C5′), 47.9 (C7′), 47.7 (C2′), 38.9 (C6′), 11.2 (T-*C*H_3). MALDI-TOF *m*/*z*: $[M + Na]^+$, found 582.185, calcd 582.183.

(1*R*,3*R*,4*R*,5*R*,7*S*)-1-(4,4′-Dimethoxytrityloxymethyl)-7-hydroxyl-5-trifluoroacetoxyamino-3-(thymin-1-yl)-2-oxa-bicyclo[2.2.1]-heptane (20a). To a solution of **19a** (140 mg, 0.25 mmol) in dry ethanol (5 mL) was added 20% $Pd(OH)_2$/C (108 mg) and cyclohexene (2 mL). The mixture was refluxed overnight and then filtered through a Celite pad, and the organic solvent was evaporated to dryness. The residue was coevaperated with dry pyridine twice and dissolved in the same solvent. 4,4′-Dimethoxytrityl chloride (154 mg, 0.45 mmol) was added and the mixture was stirred overnight at rt.The solvent was removed . The residue was diluted with DCM, washed with saturated $NaHCO_3$. The oganic layer was separated, dried over $MgSO_4$, and evaporated. The residue was applied to column chromatography on silica gel (0.5−1% methanol in DCM containing 1% pyridine) to give **20a** (111 mg, 65% in two steps). ^{1}H NMR (500 MHz, CD-Cl_3+DABCO): δ 7.70 (1H, s, H6), 7.45 (2H, d, *J* = 7.5 Hz, aromatic), 7.34−7.19 (8H, m, aromatic and N*H*), 6.84 (4H, d, *J* = 7.5 Hz, aromatic), 5.81 (1H, s, H1′), 4.79 (1H, m, H7′), 4.37 (1H, s, H3′), 3.79 (6H, s, 2xOCH_3), 3.54 (1H, d, J_{gem} = 11 Hz, H5′), 3.36 (1H, d, J_{gem} = 11 Hz, H5″), 2.93 (1H, d, $J_{2',7'}$ = 4.0 Hz, H2′), 2.80 (s, DABCO), 2.37 (1H, dd, J_{gem} = 14 Hz, $J_{6',7'}$ = 10.0 Hz, H6′), 1.62 (T-CH_3), 1.52 (1H, dd, J_{gem} = 14 Hz, $J_{6'',7'}$ = 4.5 Hz, H6″). ^{13}C NMR (125 MHz, $CDCl_3$+DABCO): δ 163.4 (C4), 157.7 (aromatic), 156.5 (q, *J* = 36 Hz, *C*OCF_3), 149.3 (C2), 143.5, 134.5 (aromatic), 134.1 (C6), 129.1, 128.0, 127.1, 127.0, 126.1 (aromatic), 113.5(q, *J* = 286 Hz, *C*F_3), 112.3 (aromatic), 109.2 (C5), 87.9 (C4′), 85.6 (DMTr-*C*), 82.0 (C1′), 71.0 (C3′), 59.7 (C5′), 54.2 (O*C*H_3), 48.6 (C2′), 46.8 (C7′), 45.8 (DABCO), 35.6 (C6′), 11.4 (T-*C*H_3). MALDI-TOF *m*/*z*: $[M + Na]^+$, found 704.198, calcd 704.220.

(1*R*,3*R*,4*R*,5*S*,7*S*)-1-(4,4′-Dimethoxytrityloxymethyl)-7-hydroxyl-5-trifluoroacetoxyamino-3-(thymin-1-yl)-2-oxa-bicyclo[2.2.1]-heptane (20b). Compound **20b** (37 mg, 60% in two steps) was obtained from **19b** after following the same reaction and workup procedure as **20a**. ^{1}H NMR (500 MHz, $CDCl_3$+DABCO): δ 7.75 (1H, s, H6), 7.58 (1H, d, $J_{NH,H7'}$ = 9.5 Hz, N*H*), 7.44 (2H, d, *J* = 7.5 Hz, aromatic), 7.33−7.25 (7H, m, aromatic), 6.85 (4H, m, aromatic), 5.41 (1H, s, H1′), 4.60 (1H, m, H7′), 4.37 (1H, s, H3′), 3.80 (6H, s, 2xOCH_3), 3.67 (1H, d, J_{gem} = 11 Hz, H5′), 3.39 (1H, d, J_{gem} = 11 Hz, H5″), 2.80 (s, DABCO), 2.68 (1H, s, H2′), 2.26 (1H, dd, J_{gem} = 13.5 Hz, $J_{6',7'}$ = 8.5 Hz, H6′), 1.65 (1H, dd, J_{gem} = 13.5 Hz, $J_{6'',7'}$ = 3.2 Hz, H6″),1.58 (T-CH_3). ^{13}C NMR (125 MHz, $CDCl_3$+DABCO): δ 163.0 (C4), 157.8 (aromatic), 155.5 (q, *J* = 36 Hz, *C*OCF_3), 149.0, 148.8 (aromatic), 143.4 (C2), 135.0,

134.4 (aromatic), 133.9 (C6), 129.1, 129.0, 126.3, 122.8 (aromatic), 113.5(q, J=286 Hz, CF_3), 112.3 (aromatic), 108.9 (C5), 88.0 (C4′), 85.9 (DMTr-C), 84.8 (C1′), 71.6 (C3′), 59.4 (C5′), 54.3 (OCH_3), 49.2 (C2′), 47.8 (C7′), 45.8 (DABCO), 38.9 (C6′), 11.4 (T-CH_3). MALDI-TOF m/z: $[M + Na]^+$, found 704.196, calcd 704.220.

(1*R*,3*R*,4*R*,7*S*)-7-Benzyloxy-1-benzyloxymethyl-3-(thymin-1-yl)-2-oxa-bicyclo[2.2.1]heptan-5-one Oxime (5). To a solution of **2a** (1.4 g, 2.45 mmol) in ethyl acetate (50 mL) were added K_2CO_3 (814 mg, 5.92 mmol) and 77% 3-chloroperbenzoic acid (mCPBA, 665 mg, 2.98 mmol). After stirring at rt for 1 h, the white suspension was diluted with ethyl acetate and washed with water. The organic layer was separated, dried over $MgSO_4$, and evaporated. The residue was chromatographed over silica gel (0.8−2% methanol in DCM) to give compound **5** (702 mg, 60%). ^{1}H NMR (500 MHz, $CDCl_3$): δ 8.82 (1H, broad, OH), 8.19 (1H, broad, NH), 7.69 (1H, s, H6), 7.37−7.24 (10H, m, aromatic), 5.64 (1H, s, H1′), 4.64−4.59 (3H, m, CH_2Bn), 4.76 (1H, d, J_{gem} = 9.5 Hz, CH_2Bn), 4.21 (1H, s, H3′), 3.95 (1H, d, J_{gem} = 9.5 Hz, H5′), 2.55 (1H, d, J_{gem} = 9.5 Hz, H5″), 3.60 (1H, s, H2′), 2.72 (1H, d, J_{gem} = 14.5 Hz, H6′), 2.55 (1H, d, J_{gem} = 14.5 Hz, H6″), 1.54(3H, s, T-CH_3). ^{13}C NMR (125 MHz, $CDCl_3$): δ 162.9 (C4), 156.9 (C7′), 148.7 (C2), 136.4, 135.8 (aromatic), 134.6 (C6), 127.6, 127.4, 127.1, 126.8, 126.7 (aromatic), 108.7 (C5), 87.3 (C4′), 84.6 (C1′), 76.3 (C3′), 72.82 (CH$_2$Bn), 71.1 (CH$_2$Bn), 65.8 (C5′), 49.2 (C2′), 33.4 (C6′), 11.1 (T-CH$_3$). MALDI-TOF m/z: $[M + Na]^+$, found 500.210, calcd 500.180.

(1*R*,3*R*,4*R*,5*S*,7*S*)-7-Benzyloxy-1-benzyloxymethyl-5-hydroxyl-3-(thymin-1-yl)-2-oxa-bicyclo[2.2.1]heptane (7). To a solution of compound **5** (580 mg, 1.21 mmol) and NaOAc (36 mg) in dry DCM (55 mL) was added 0.3 M Dess-Martin periodinate solution in DCM (5.44 mL, 1.63 mmol) dropwise. After stirring at rt for 30 min, the mixture was diluted with DCM and washed with saturated $NaHCO_3$. The organic solvent was dried over $MgSO_4$ and evaporated to dryness to give crude compound **6**, which was dissolved in ethanol (15 mL). $NaBH_4$ (187 mg, 4.89 mmol) was added to the solution. After stirring at rt for 3 h, the solvent was removed, and the residue was diluted with DCM and washed with saturated $NaHCO_3$. The organic layer was separated, dried over $MgSO_4$, and then evaporated. The residue was chromatographed over silica gel (0.5−2% methanol in DCM) to give compound **7** (226 mg, 40% in two steps). ^{1}H NMR (600 MHz, $CDCl_3$): δ 8.21 (1H, broad, NH), 7.64 (1H, s, H6), 7.39−7.25 (10H, m, aromatic), 5.32 (1H, s, H1′), 4.64 (2H, d, J_{gem} = 11.4 Hz, CH_2Bn), 4.59 (2H, d, J_{gem} = 11.4 Hz, CH_2Bn), 4.29 (1H, app t, J = 9.6 Hz, H7′), 4.16 (1H, s, H3′), 3.88 (1H, d, J_{gem} = 11.4 Hz, H5′), 3.84 (1H, d, J_{gem} = 11.4 Hz, H5″), 2.82 (1H, s, H2′), 2.78 (1H, d, $J_{7',OH}$ = 11.4 Hz, OH), 2.32 (1H, dd, J_{gem} = 13.8 Hz, $J_{6',7'}$ = 7.8 Hz, H6′), 1.82 (1H, dd, J_{gem} = 13.8 Hz, $J_{6',7'}$ = 2.4 Hz, H6″), 1.6 (3H, s, T-CH_3). ^{13}C NMR (125 MHz, $CDCl_3$): δ 162.5 (C4), 148.6 (C2), 136.5, 135.5 (aromatic), 134.6 (C6), 127.7, 127.6, 127.4, 127.1, 126.8 (aromatic), 108.5 (C5), 87.0 (C4′), 83.6 (C1′), 78.1 (C3′), 72.7 (CH$_2$Bn), 72.2 (CH$_2$Bn), 71.3 (C7′), 66.2 (C5′), 49.0 (C2′), 42.0 (C6′), 11.2 (T-CH$_3$). MALDI-TOF m/z: $[M+Na]^+$, found 487.180, calcd 487.185.

(1*R*,3*R*,4*R*,5*S*,7*S*)-7-Benzyloxy-1-benzyloxymethyl-5-((methylthio)thiocarbonyl)oxy-3-(thymin-1-yl)-2-oxa-bicyclo[2.2.1]heptane (22). To a solution of compound **7** (190 mg, 0.41 mmol) in dry THF (6 mL) was added 60% NaH (50 mg, 1.22 mmol) at 0 °C. After stirring at rt for 1 h, CS_2 (190 μL, 4.1 mmol) was added to the suspension at 0 °C, and the resulting mixture was stirred at rt for 30 min and then at 40 °C for 2 h. The solution became clear and was cooled by ice. Methyl iodide (163 μL, 2.61 mmol) was added at 0 °C, and the mixture was stirred at rt for another 3 h. The reaction was quenched by chilled water and extracted with ethyl acetate several times. The organic layer was dried over $MgSO_4$ and evaporated. The residue was chromatographed over silica gel (20−50% ethyl acetate in cyclohexane) to give compound **22** (152 mg, 65%). ^{1}H NMR (500 MHz, $CDCl_3$): δ 8.40 (1H, s, NH), 7.66 (1H, s, H6), 7.36−7.30 (10H, m, aromatic), 5.78 (1H, dd, $J_{6',7'}$ = 6 Hz, $J_{6'',7'}$ = 3 Hz, H7′), 5.48 (1H, s, H1′), 4.66 (1H, d, J_{gem} = 9.5 Hz, CH_2Bn), 4.60 (2H, 2xd, J_{gem} = 9.5 Hz, CH_2Bn), 4.43 (1H, d, J_{gem} = 9.5 Hz, CH_2Bn), 4.10 (1H, s, H3′), 3.85 (1H, d, J_{gem} = 9 Hz, H5′), 3.82 (1H, d, J_{gem} = 9 Hz, H5″), 3.27 (1H, s, H2′), 2.51 (3H, s, SCH_3), 2.44 (1H, dd, J_{gem} = 11.5 Hz, $J_{6',7'}$ = 6 Hz, H6′), 2.15 (1H, dd, J_{gem} = 11.5 Hz, $J_{6'',7'}$ = 3 Hz, H6″), 1.53 (T-CH_3). ^{13}C NMR (125 MHz, $CDCl_3$): δ 213.7 (C═S), 162.6 (C4), 148.7 (C2), 136.6, 136.1 (aromatic), 134.6 (C6), 127.6, 127.4, 127.0, 126.9, 126.8 (aromatic), 108.6 (C5), 87.2 (C4′), 84.0 (C1′), 80.4 (C7′), 76.5 (C3′), 72.8 (CH$_2$Bn), 71.0 (CH$_2$Bn), 65.6 (C5′), 46.4 (C2′), 39.1 (C6′), 18.2 (SCH_3), 11.1 (T-CH$_3$). MALDI-TOF m/z: $[M + H]^+$, found 555.158, calcd 555.162.

(1*R*,3*R*,4*R*,7*S*)-7-Benzyloxy-1-benzyloxymethyl-3-(thymin-1-yl)-2-oxa-bicyclo[2.2.1]heptane (1). Compound **22** (150 mg, 0.27 mmol) was dissolved in dry toluene (6 mL) and purged with dry nitrogen for 30 min. AIBN (10 mg, 0.06 mmol) and nBu$_3$SnH (216 μL, 0.8 mmol) were added, and the mixture was refluxed for 1.5 h. The mixture was cooled to rt. After evaporation of the solvent, the residue was chromatographed over silica gel (25−50% ethyl acetate in cyclohexane) to give compound **1** (72 mg, 65%). ^{1}H NMR (600 MHz, $CDCl_3$): δ 8.40 (1H, broad, NH), 7.74 (1H, s, H6), 7.36−7.27 (10H, m, aromatic), 5.47 (1H, s, H1′), 4.61 (2H, 2xd, J_{gem} = 11.4 Hz, CH_2Bn), 4.55 (1H, d, J_{gem} = 11.4 Hz, CH_2Bn), 4.48 (1H, d, J_{gem} = 11.4 Hz, CH_2Bn), 3.99 (1H, s, H3′), 3.86 (1H, d, J_{gem} = 10.8 Hz, H5′), 3.78 (1H, d, J_{gem} = 10.8 Hz, H5″), 2.75 (1H, d, $J_{2',7'}$ = 4.2 Hz, H2′), 2.07 (1H, tt, $J_{2',7'}$ = 4.2 Hz, $J_{6'',7'}$ = 4 Hz, $J_{6',7'}$ = 12 Hz, $J_{7'',7'}$ = 12 Hz, H7′), 1.88 (1H, dt, $J_{6',7''}$ = 4 Hz, $J_{6',7'}$ = 12 Hz, $J_{6',6''}$ = 12 Hz, H6′), 1.73 (1H, ddd, $J_{6',7''}$ = 4 Hz, $J_{6'',7''}$ = 8.6 Hz, $J_{7',7''}$ = 12 Hz, H7″), 1.64 (1H, ddd, $J_{6'',7''}$ = 8.6 Hz, $J_{6'',7'}$ = 4 Hz, $J_{6',6''}$ = 12 Hz, H6″), 1.57 (T-CH_3). ^{13}C NMR (125 MHz, $CDCl_3$): δ 162.8 (C4), 148.9 (C2), 136.8, 136.6 (aromatic), 135.1 (C6), 127.5, 127.4, 127.0, 126.9, 126.7,126.5 (aromatic), 108.1 (C5), 87.3 (C4′), 87.2 (C1′), 76.5 (C3′), 72.7 (CH$_2$Bn), 70.9 (CH$_2$Bn), 66.6 (C5′), 42.7 (C2′), 28.5 (C6′), 22.1 (C7′), 11.1 (T-CH$_3$). MALDI-TOF m/z: $[M + H]^+$, found 449.210, calcd 449.208.

(1*R*,3*R*,4*R*,7*S*)-1-(4,4′-Dimethoxytrityloxymethyl)-7-hydroxyl-3-(thymin-1-yl)-2-oxa-bicyclo[2.2.1]heptane (23). To a solution of **1** (64 mg, 0.14 mmol) in dry methanol (4 mL) were added 20% $Pd(OH)_2$/C (72 mg) and ammonium formate (182 mg, 2.8 mmol). The mixture was refluxed for 2 h and then filtered through a Celite pad, and the organic solvent was evaporated to dryness. The residue was coevaperated with dry pyridine twice and dissolved in the same solvent. 4,4′-Dimethoxytrityl chloride (96 mg, 0.28 mmol) was added, and the resulting mixture was stirred overnight at rt. After the solvent was removed, the residue was diluted with DCM and washed with saturated $NaHCO_3$. The organic layer was dried over $MgSO_4$ and evaperated, and the residue was applied to column chromatography on silica gel (0.5−1% methanol in DCM containing 1% pyridine) to give **23** (56 mg, 70% in two steps). ^{1}H NMR (500 MHz, $CDCl_3$ + DABCO): δ 7.80 (1H, s, H6), 7.45 (2H, d, J = 7.5 Hz, aromatic), 7.37−7.16 (7H, m, aromatic), 6.85 (4H, m, aromatic), 5.40 (1H, s, H1′), 4.22 (1H, s, H3′), 3.80 (6H, s, 2xOCH_3), 3.64 (1H, d, J_{gem} = 11 Hz, H5′), 3.35 (1H, d, J_{gem} = 11 Hz, H5″), 2.79 (s, DABCO), 2.63 (1H, d, $J_{2',7'}$ = 3 Hz, H2′), 2.08 (1H, m, H7′), 1.74 (2H, m, H6′, H7″), 1.60 (T-CH_3), 1.58 (1H, m, H6″). ^{13}C NMR (125 MHz, $CDCl_3$ + DABCO): δ 162.9 (C4), 157.7 (aromatic), 149.0 (C2), 143.6 (aromatic), 134.6 (C6), 129.0, 128.0, 127.2, 127.0, 126.1, 124.3, 112.3(aromatic), 108.4 (C5), 87.9 (C4′), 87.4 (C1′), 85.7 (DMTr-C), 70.9 (C3′), 60.0 (C5′), 54.2 (OCH$_3$), 46.0 (DABCO), 45.1 (C2′), 28.2 (C6′), 22.1 (C7′), 11.4 (T-CH$_3$). MALDI-TOF m/z: $[M + Na]^+$, found 593.198, calcd 593.226.

General Procedure for Phosphoramidite Synthesis. To a solution of substrate (1 equiv) in dry DCM were added DIPEA (5 equiv) and 2-cyanoethyl N,N-diisopropyl phosphoramidochloridite (3 equiv) dropwise in an ice bath. The reaction was allowed

to warm to rt and stirred at this temperature for 3 h. After being quenched with methanol, the mixture was diluted with ethyl acetate, washed with saturated $NaHCO_3$ solution, dried over $MgSO_4$, and concentrated. The residue was applied to short column chromatography on silica gel to give phosphoramidite, which was first precipitated in *n*-hexane and then dried over P_2O_5 on vacuum for three days before it was used for DNA synthesis.

Oligonucleotide Synthesis and Purification. All AONs were synthesized using an automated DNA/RNA synthesizer based on phosphoramidite chemistry. For native A, G, and C building blcok, fast deprotecting phosphoramidites (Ac for C, *i*Pr-Pac for G, Pac for A) were used. Standard DNA synthesis reagents and cycle were used except that 0.25 M 5-ethylthio-1*H*-tetrazole was used as the activator and Tac_2O as the cap A. For incorporating modified nucleotides, extended coupling time (10 min comparing to 25 s for native nucleotides) was used. Cleavage from the support and deprotection were carried out by treating the solid support with 33% aqueous ammonia at rt for 12 h to obtain the fully deprotected AONs **2**−**21**, which were purified by denaturing PAGE (20% polyacrylamide with 7 M urea), extracted with 0.3 M NaOAc, and desalted with a C-18 reverse phase cartridge to give AONs in >99% purity. Correct masses have been obtained by MALDI-TOF mass spectroscopy for each of them (Table SII.1).

The complementary RNA was also synthesized by solid-supported phosphoramidite approach based on the 2′-*O*-TEM strategy.[50,51]

UV Melting Experiments. Determination of the T_m of the AON/RNA hybrids or AON/DNA duplex was carried out in the following buffer: 60 mM Tris-HCl (pH 7.5), 60 mM KCl, 0.8 mM $MgCl_2$. Absorbance was monitored at 260 nm in the temperature range from 20 to 70 °C using an UV spectrophotometer equipped with a Peltier temperature programmer with the heating rate of 1 °C/min. Prior to measurements, the samples (1 μM of AON and 1 μM cDNA or RNA mixture) were preannealed by heating to 80 °C for 5 min followed by slow cooling to 21 °C and 30 min equilibration at this temperature. The value of T_m is the average of two or three independent measurements. If error of the first two measurements was > ±0.3 °C, the third measurement was carried out to check if the error is indeed within ±0.3 °C; otherwise it was repeated.

^{32}P Labeling of Oligonucleotides. The oligoribonucleotides and oligodeoxyribonucleotides were 5′-end labeled with ^{32}P using T4 polynucleotide kinase, [γ-^{32}P]ATP, and the standard protocol. Labeled AONs and the target RNA were purified by QIAquick Nucleotide Removal Kit, and specific activities were measured using a Beckman LS 3801 counter.

SVPDE Degradation Studies. Stability of the AONs toward 3′-exonucleases was tested using phosphodiesterase I from *Crotalus adamanteus* (obtained from USB corporation, Cleveland, OH). All reactions were performed at 3 μM DNA concentration (5′-end ^{32}P-labeled with specific activity 80,000 cpm) in 100 mM Tris-HCl (pH 8.0) and 15 mM $MgCl_2$ at 21 °C. An exonuclease concentration of 6.7 or 2.2 ng/μL was used for digestion of oligonucleotides. Total reaction volume was 30 μL. Aliquots (3 μL) were taken at proper time points and quenched by addition of stop solution (4 μL) [containing 0.05 M EDTA, 0.05% (w/v) bromophenol blue, and 0.05% (w/v) xylene cyanole in 80% formamide]. Reaction progress was monitored by 20% denaturing (7 M urea) PAGE and autoradiography.

Stability Studies in Human Blood Serum. AONs at 2 μM concentration (5′-end ^{32}P-labeled with specific activity 80,000 cpm) were incubated in 10 μL of human blood serum (male AB, obtained from Sigma-Aldrich) at 21 °C (total reaction volume was 36 μL). Aliquots (3 μL) were taken at proper time points and quenched with 4 μL of stop solution [containing 0.05 M EDTA, 0.05% (w/v) bromophenol blue, and 0.05% (w/v) xylene cyanole in 80% formamide], resolved in 20% polyacrylamide denaturing (7 M urea) gel electrophoresis, and visualized by autoradiography.

RNase H Digestion Assay. Target 0.1 μM RNA (specific activity 80 000 cpm) and AON (2 μM) were incubated in a buffer containing 20 mM Tris-HCl (pH 7.5), 20 mM KCl, 10 mM $MgCl_2$, 0.1 mM EDTA, and 0.1 mM DTT at 21 °C in the presence of 0.08 U of *E. coli* RNase H (obtained from USB corporation, Cleveland, OH). Prior to the addition of the enzyme, reaction components were preannealed in the reaction buffer by heating at 80 °C for 5 min followed by slow cooling to 21 °C and 30 min equilibration at this temperature. Total reaction volume was 30 μL. Aliquots of 3 μL were removed after 5, 10, 15, 30, and 60 min, and the reactions were terminated by mixing with stop solution [containing 0.05 M EDTA, 0.05% (w/v) bromophenol blue, and 0.05% (w/v) xylene cyanole in 80% formamide]. The samples were subjected to 20% 7 M urea PAGE and visualized by autoradiography. Pseudo-first-order reaction rates could be obtained by fitting the digestion curves to single-exponential decay functions.

Acknowledgment. Generous financial support from the Swedish Natural Science Research Council (Vetenskapsrådet), the Swedish Foundation for Strategic Research (Stiftelsen för Strategisk Forskning), and the EU-FP6 funded RIGHT project (Project no. LSHB-CT-2004-005276) is gratefully acknowledged.

Supporting Information Available: ^{1}H, ^{13}C, ^{31}P, DEPT, COSY, HMQC, HMBC of carba-LNA derivatives (SI part I); 1D NOE spectra, experimental and calculated coupling constants of key intermediates **2a**, **2b**, **1**, **4a**, and **4b** (SI part II); autoradiograms of 20% denaturing PAGE as well as degradation curves, showing the cleavage kinetics of target RNA in AON/RNA hybrides by *E. coli* RNase H1, the detailed discussion about the structure−activity relationships of all modified carba-LNAs and carba-ENAs for thermal affinity, nuclease stability and the RNase recruitment of DNA/RNA duplexes, all individual reaction steps, workup, and product characterization for the intermediates in Scheme 3 and the characterization for final amidites **21a**,**b**, **24**, **31a**,**b** (SI part II). These materials are available free of charge via the Internet at http://pubs.acs.org.

(50) Zhou, C.; Honcharenko, D.; Chattopadhyaya, J. *Org. Biomol. Chem.* **2007**, *5*, 333–343.
(51) Zhou, C.; Pathmasiri, W.; Honcharenko, D.; Chatterjee, S.; Barman, J.; Chattopadhyaya, J. *Can. J. Chem.* **2007**, *85*, 293–301.